Coordination Chemistry Reviews 275 (2014) 1–18

Contents lists available at ScienceDirect

Coordination Chemistry Reviews

journal homepage: www.elsevier.com/locate/ccr

Review

Recent developments in the crystal engineering of diverse coordination modes (0–12) for Keggin-type polyoxometalates in hybrid inorganic–organic architectures

Masoud Mirzaei [a,*], Hossein Eshtiagh-Hosseini [a], Mahboubeh Alipour [a], Antonio Frontera [b]

[a] Department of Chemistry, Ferdowsi University of Mashhad, Mashhad 917751436, Iran
[b] Departament de Química, Universitat de les Illes Balears, Crta. de Valldemossa km 7.5, Palma de Mallorca, Baleares E-07122, Spain

Contents

ARTICLE INFO

Article history:
Received 16 December 2013
Accepted 12 March 2014
Available online 23 April 2014

Keywords:
Coordination mode
Crystal engineering
Hybrid inorganic–organic
Keggin
Polyoxometalate
Supramolecular chemistry

ABSTRACT

At present, research into polyoxometalates (POMs) is a hot topic in many scientific fields, mainly because of their vast range of potential applications. Recently, the coordination ability of POMs has attracted the attention of the scientific community because it allows them to behave as unusual inorganic ligands. A direct consequence of this ability is the assembly of high-dimensional architectures, which have been reported during the past decade. Thus, the present review considers the latest achievements in the construction of inorganic–organic hybrid materials based on POMs, with a specific focus on their various coordination modes, particularly Keggin-type anions, which are widely available. First, this huge family of compounds is classified based on the number of components in the system. Second, recent research into organic N and O-donor ligands is described.

1. Introduction

Polyoxometalates (POMs) are discrete anionic metal–oxygen clusters, which exhibit a great diversity of sizes, nuclearities, and shapes. The metal (M) is an early transition metal in a high oxidation state, usually $V^{IV,V}$, Mo^{VI}, or W^{VI} [1]. These species have been known for almost two centuries and they have attracted much interest because of their applications in various research areas, including magnetism [2], sensing [3], catalysis, and medicine [4]. The applications of POMs are based mostly on their ability to stabilize anions with charges ranging from −3 to −14 [5]. During the last decade, the POMs research field has developed rapidly because of the increasing availability of single crystal data collection strategies. In particular, an emerging multidisciplinary research area in POM chemistry is the synthesis of inorganic–organic hybrids [6]. The strategy used for the functionalization of POMs with organic-containing species can be either covalent or noncovalent, which increases the potential to generate new compounds

* Corresponding author. Tel.: +98 05118797022; fax: +98 05118796416.
E-mail address: mirzaeesh@um.ac.ir (M. Mirzaei).

http://dx.doi.org/10.1016/j.ccr.2014.03.012
0010-8545/

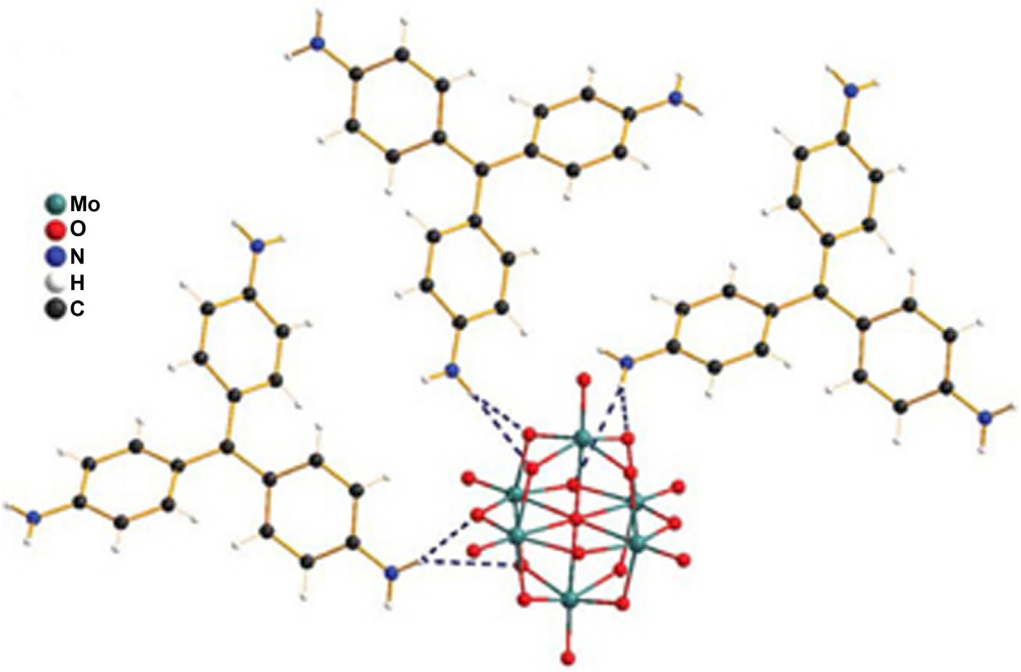

Fig. 1. Representation of charge-assisted N—H···O hydrogen bonding interactions in the compound $[PR]_2[Mo_6O_{19}]\cdot 6dmf$ [22].

in this already huge family that have new topologies and high-dimensional extended architectures with modified properties [7]. In the near future, it is likely that hundreds of new compounds will be synthesized, some of which will have novel properties. Clearly, more research is needed to facilitate the control of synthesis, including selecting appropriate POM building blocks and organic components. In recent years, several studies have systemically characterized the effects of different factors on the final structure of POM-based hybrids, including the size [8] and charge [9] of POMs, temperature [10], pH [11], the use of flexible or rigid organic ligands [12], and influence of a second transition metal [13]. Thus, the intelligent choice of POMs and other components may facilitate the production of new materials with fascinating structures and properties. Moreover, recent studies have also contributed to our understanding of the coordination abilities of POMs and the effects of intermolecular interactions on their solid state architecture [14–16]. Similarly, the effects of hybrid inorganic–organic materials on crystal packing have been investigated [17–20]. In addition, the coordination properties of POMs are very difficult to envisage compared with other organic ligands, thus the behavior of POMs is unpredictable. The aim of this review is to provide an overview of the different behaviors of POMs and to select the most relevant studies that have contributed to recent developments in this area. First, a classification of POM-based hybrids based on the number of components in the system is provided. Next, the coordination ability of POMs is considered, which makes them behave as unusual inorganic ligands. The recent use of three different families of organic ligands is reviewed in the final section.

2. Classification of polyoxometalate-based inorganic–organic hybrids

Inorganic–organic hybrids compounds based on POMs can be classified conveniently into two main classes, which depend on the number of components in the system.

2.1. Class I: two-component systems

Class I systems comprise a combination of a POM and an organic component, which can adopt two main different roles depending on its structure and charge, i.e., it either acts as a charge-compensating, space-filling, and structure-directing cation, or it is bonded directly to the POM. The anionic character of POMs naturally allows their association with organic countercations to form Class I hybrids, but the organic ligand can substitute for an oxo group of the POM and be linked directly to the metallic center. A comprehensive review of this particular topic has been published recently [21]. However, some recent examples involving inorganic–organic hybrid dyes, such as salts containing triarylmethane cations and hexametalates $[M_6O_{19}]^{2-}$ (M = Mo, W), have also been mentioned [22]. A number of charge-assisted hydrogen bonds N—H···O exist between the cation —NH_2 functions and anionic oxygen atoms, which can facilitate crystallinity in the solid state. Interestingly, the solubility can be improved by appropriate ring substitutions (Fig. 1). Inexpensive triarylmethane dye cations have promising properties as visible energy transfer agents for POM anions because of their intense absorption in the visible region, which can be tuned by ring substitution.

The hybridization of organic chromophores with POM can also enhance the two-photon absorption cross-sections and thermal stability in trans-4-(4′-(N,N-dialkylaminostyryl))-N-methylpyridinium $[Mo_6O_{19}]^{2-}$ [23]. All of these the structures have similar characteristics, where the cations interact with the anions via electrostatic attraction, as well as via C—H···O hydrogen bonds and other intermolecular interactions between the cations, e.g., π–π stacking interactions. Furthermore, the properties of the Dawson-type molybdosulfate and methylene blue (organic dye) $(MB)_5[S_2Mo_1{}^{V}Mo_{17}{}^{VI}O_{62}]\cdot CH_3CN$ ($MB = C_{16}H_{18}N_3S$) have been studied, which share similar features [24]. X-ray diffraction analysis showed that the polyoxoanions fill the interspace formed by the MB cations and acetonitrile, and they interact via Coulombic forces and a variety of hydrogen bonds, such as C—H···O, C—H···S, C—H···N, C—H···π, and π–π stacking interactions. Studies of their photoluminescent properties in acetonitrile solution

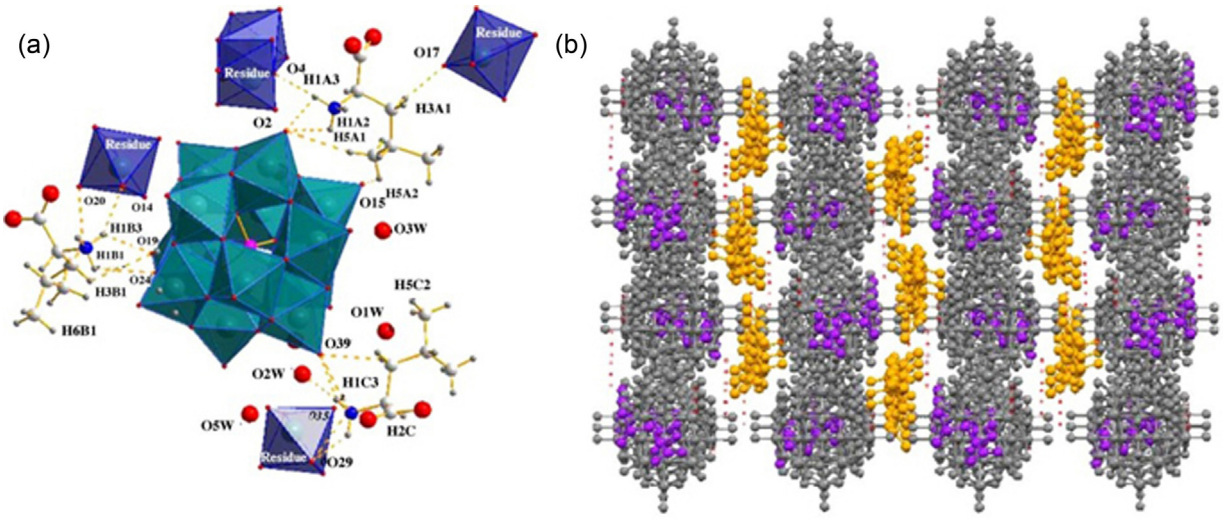

Fig. 2. (a) Chemical environment of the $[(PO_4)W_{12}O_{36}]^{3-}$ anion. The dashed orange lines indicate the hydrogen bond interactions of the three D/L-leucinium$^+$ ions (the residues represent neighboring Keggin anions). (b) The three-dimensional layered structure along the *a*-axis [31].

suggest the presence of ion pairs of $[S_2Mo_{18}O_{62}]^{4-}$ anions and MB cations, or charge-transfer transitions between the cationic MB donor and the POM acceptor. Another family of organic compounds used to construct hybrid POMs are amino acids, where proline [25–27], glycine [27–30], leucine [31–33], and asparagine [33] are combined with POMs to produce POM-amino acid hybrids with promising biological applications. Interestingly, chiral compounds have been obtained in some cases [25,27]. For example, the compound [D/L-leucinium]$_3[(PO_4)W_{12}O_{36}]\cdot 4.5H_2O$ with a centric space group ($P2_1/c$) has been synthesized successfully [31], where there is a complex network of hydrogen bonding interactions between D/L-Leu$^+$ and water molecules with the $[(PO_4)W_{12}O_{36}]^{3-}$ cluster (Fig. 2a). The most unique feature of this structure is its three-dimensional (3D) inorganic infinite tunnel-like framework, which results in a weak interlayer interaction (Fig. 2b) and it provides a desirable condition for exploring its potential as a host in a host–guest assembly.

Recently, a template-directing effect of anionic POM clusters in Class I was achieved using flexible organic cations in three hybrid compounds [34]. In the first compound, $(H_2bpp)(Hbpp)[PMo_{12}O_{40}]\cdot 3DMF$ (bpp = 1,3-bis(4-pyridyl)propane), the 3D architecture is dominated by the self-directing effects of supramolecular interactions between the inorganic clusters and protonated organic cations, thereby generating small distances between two neighboring Keggin clusters. In addition to these strong interactions, other weaker intermolecular hydrogen bonds modulate the final solid state geometry. The N···O distances are 2.68(3)–2.73(4) Å, which indicate strong hydrogen bonding interactions. As shown in Fig. 3, organic cations wrap Keggin anions to form an inclusion complex that measures ca 2 nm.

The aforementioned POM-based hybrids have functional subunits with electrostatic interactions. As mentioned in the introduction, another approach is to develop POM-based networks that are functionalized directly by the organic species. Chemically grafting organic ligands onto POMs can maintain, modify, or enhance the optical, electrical, thermal, and fluorescence properties of the POMs. Two inorganic–organic hybrid clusters with one or two covalently linked pyrene fluorescent tails were synthesized from a Lindqvist type polyoxovanadate head cluster via triester capping groups, which offered a unique opportunity

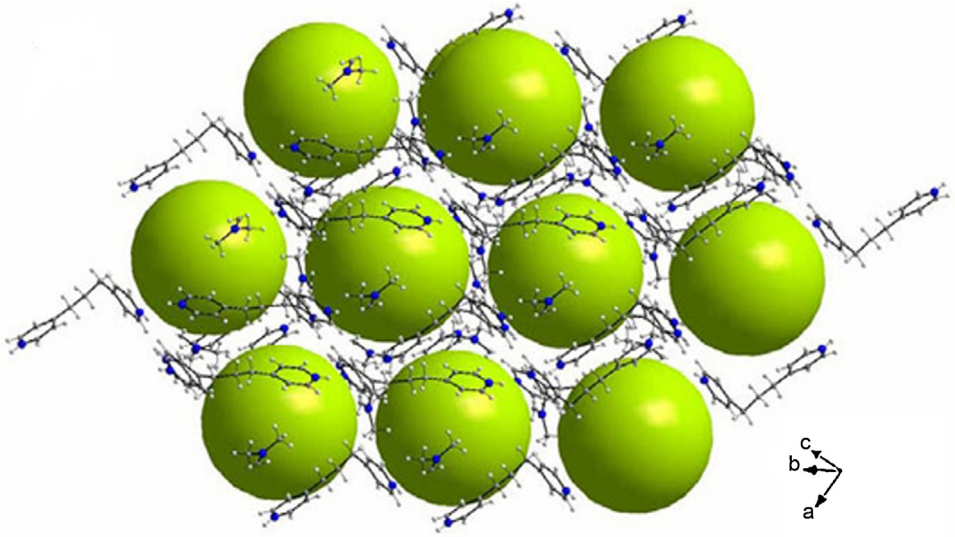

Fig. 3. Representation of the inclusion of a $[PMo_{12}O_{40}]^{3-}$ anion (drawn as a ball) in a packing view, which shows the directing effect of anions [34].

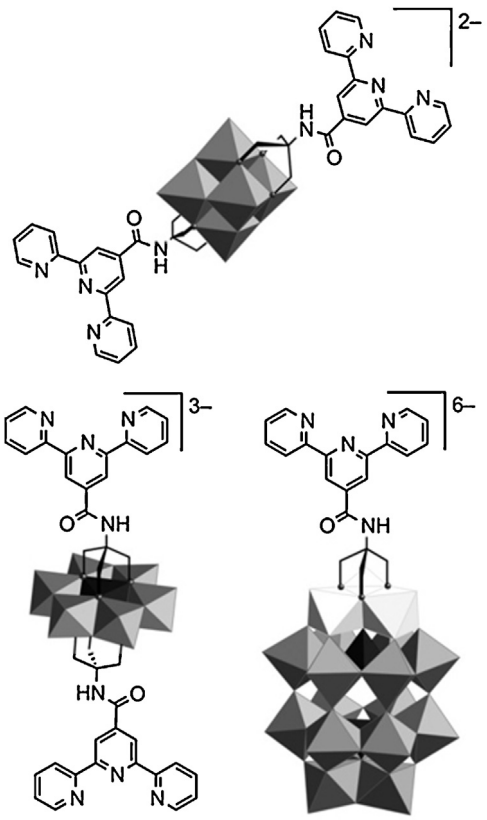

Fig. 4. Terpyridine-functionalized POMs [36].

to study the interactions between the hybrid clusters and their counterions [35]. Four different counterions, i.e., TBA^+, TEA^+, TMA^+ (tetrabutyl ammonium, tetraethylammonium, and tetramethylammonium respectively), and H^+, were used to study their effects on the vesicular structures and their consequent roles in the fluorescent properties of the pyrene groups on vesicle surfaces. By replacing the TBA^+ counterions with protons, the new vesicles exhibited interesting pH-dependent fluorescence properties. Terpyridine functionalized POMs were also obtained using a modular strategy by Hanan and Hasenknopf et al. based on Lindqvist, Anderson, and Dawson structures [36]. Single crystal X-ray diffraction data detected the grafted organic moiety on each oxo-cluster (Fig. 4). The use of other metal ions, ligands, and grafting functions also presents a wide range of new possibilities (see Scheme 1). As shown in the next section, the coordination of transition metal complexes (TMCs) with the oxo ligands of POMs is common, but the control of their positions is limited and

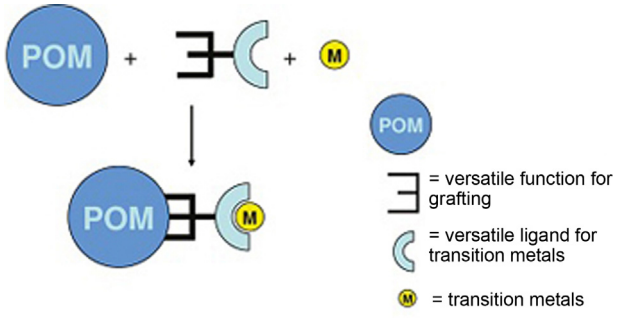

Scheme 1. Strategy for the modular assembly of transition metal functionalized POMs

Reprinted with permission from Ref. [20].

the multidimensional networks obtained are often unpredictable. Interestingly, various metals can coordinate with terpyridine coordination sites, including Ru and Pd. This combination generates charge-transfer hybrids (for Ru) or multicomponent systems (for Pd). The post-functionalization of hybrid disilylated POM platforms to photoactive ruthenium complexes has also been demonstrated for pyrene chromophores in hybrid disilylated Keggin and Dawson-type POMs in a highly efficient and modular manner [37]. The presence of the POM leads to luminescence quenching in the chromophores, which is attributed to intramolecular electron transfer from the chromophore to the POM.

In this context, a recent study described the conformational flexibility and programmed assembly of a dumbbell-shaped POM-organic hybrid molecule that comprised two Dawson-type POMs linked by a 2,2′-bipyridine unit [38]. This hybrid can coordinate with metal ions (in this case, Zn^{2+}) and it is recognized as the first example of a POM-based metal ion-driven molecular switch. In the hybrid $TBA_{10}H_2[\{P_2V_3W_{15}O_{59}(OCH_2)_3CNHCO\}_2(C_5H_3N)_2]$ (TBA, tetrabutylammonium), the POM units are connected to the 4,4′ positions of the heteroaromatic rings. Thus, the hybrid can exist in two conformations: the *trans* dumbbell in a metal ion-free environment and the *cis* dumbbell driven by the coordination of the two nitrogen atoms in the central 2,2′-bipy unit with a metal ion (Fig. 5). A multi-responsive switching behavior can be observed during the transformation process. Moreover, it has been shown that the phosphovanadotungstate polyanion $[P_2W_{15}V_3O_{62}]^{9-}$ is a powerful support for diolamide ligands and the resulting hybrids stabilize the palladacycles conjugated to the inorganic framework [39]. Density functional theory-based modeling showed that the strong electron withdrawal effect of the POM transmitted via the conjugated carbonyl was responsible for this simple insertion.

It is notable that covalently linked porphyrin-POMs can be considered as new model systems that mimic natural photosynthesis in terms of molecular engineering and new photonic properties may emerge from these constructs and materials [40]. In order to determine the possibility of electron transfer, a combination of a zinc-porphyrin photosensitizer with an Anderson-type hexamolybdate and a Dawson-type vanadotungstate was produced [41], which led to the formation of $[N(C_4H_9)_4]_3[MnMo_6O_{18}\{(OCH_2)_3CNHCO(ZnTPP)\}_2]$ and $[N(C_4H_9)_4]_5H[P_2V_3W_{15}O_{59}\{(OCH_2)_3CNHCO(ZnTPP)\}]$ with two and one pendant zinc(II)-tetraphenylporphyrins, respectively (Fig. 6). Photophysical studies demonstrated the influence of the POM on the properties of the porphyrin, i.e., communication in the excited state.

2.2. Class II: three-component systems

In Class II systems, a secondary metal (often a transition metal) is present that forms a complex, which is coordinated with the organic component. This TMC may be isolated (charge-balancing cation) or coordinated directly by the oxygen atoms of POMs, which are considered as ligands. The structures constructed from POMs and TMCs, and assembled via non-covalent supramolecular interactions, always contain two independent components: negative POMs and positive TMCs. An interesting example involves the introduction of POMs into metal–organic complex systems that contain copper ions and bichelate bridging ligands (bis(3-(2-pyridyl)pyrazole-1-ylmethyl)benzene = bppmb) [42]. The use of Keggin type POMs, $[XW_{12}O_{40}]^{n-}$ (X = B, n = 5 and X = Si, n = 4), induces the formation of a series of novel metal–organic secondary building units, such as helical chains, which also form interesting supramolecular self-assemblies with the polyoxoanions. Fig. 7 shows how ligands are linked alternately via their Cu(I) centers to form the final helical chains in the compound $[Cu^I(bppmb)]_4[SiW_{12}O_{40}]\cdot 5H_2O$. The cationic [CuL] units

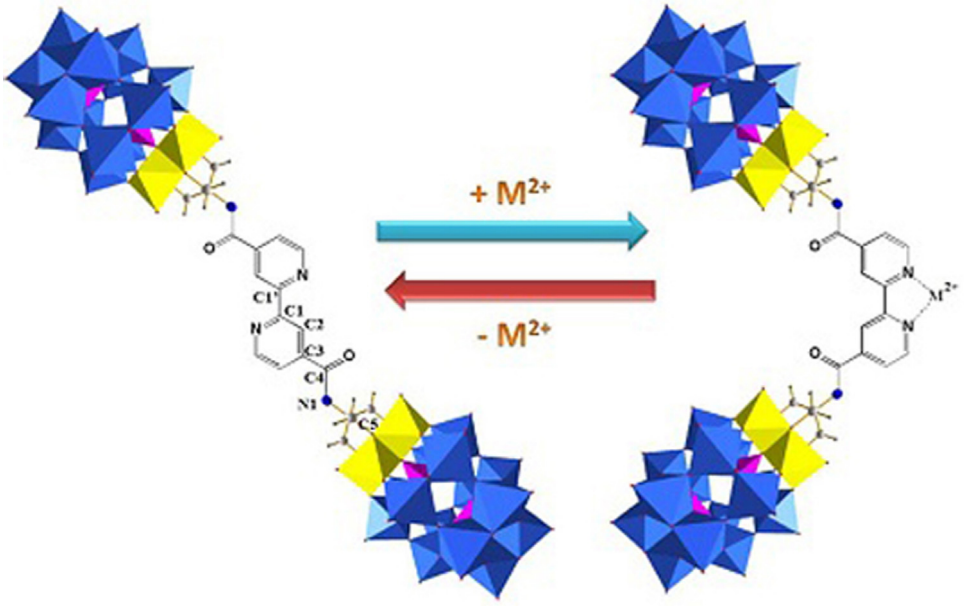

Fig. 5. The reversible conformational transformation that occurs when a *trans* dumbbell is complexed with a divalent metal chloride to form a *cis* dumbbell [38].

and the negative Keggin-type polyoxoanions stack together into a Coulombic aggregation where the adjacent [CuL] units have weak intermolecular C—H···π interactions with the C—H group in the pyrazole ring and the adjacent plane of the benzene ring.

The first example of a hybrid compound constructed from POMs and supramolecular noncovalent coordination cages, i.e., $[PW^{VI}_{10.5}W^{V}_{1.5}O_{40}][Cu(2,2'\text{-bpy})_2]_{4.5}$, was reported recently [43]. Three $[Cu_2(2,2'\text{-bpy})_2]^+$ fragments interact with each other via noncovalent interactions in an equilateral triangle cage. The packing motif of the supramolecular cages and POMs is interesting. Each cage interacts with six neighboring POMs via six C—H···O hydrogen bonds, while each POM also interacts with the three cages via C—H···O hydrogen bonds. Fig. 8 shows how these C—H···O interactions collectively facilitate the construction of a large, infinite two-dimensional (2D) layer structure along the crystallographic *ab* plane.

In addition, POMs often fill some of the pores in the coordination polymers (PCPs, also referred as metal–organic frameworks (MOFs)) to prevent the cationic polymer from self-interpenetrating. The structures of the PCPs/POM host–guest compounds mainly

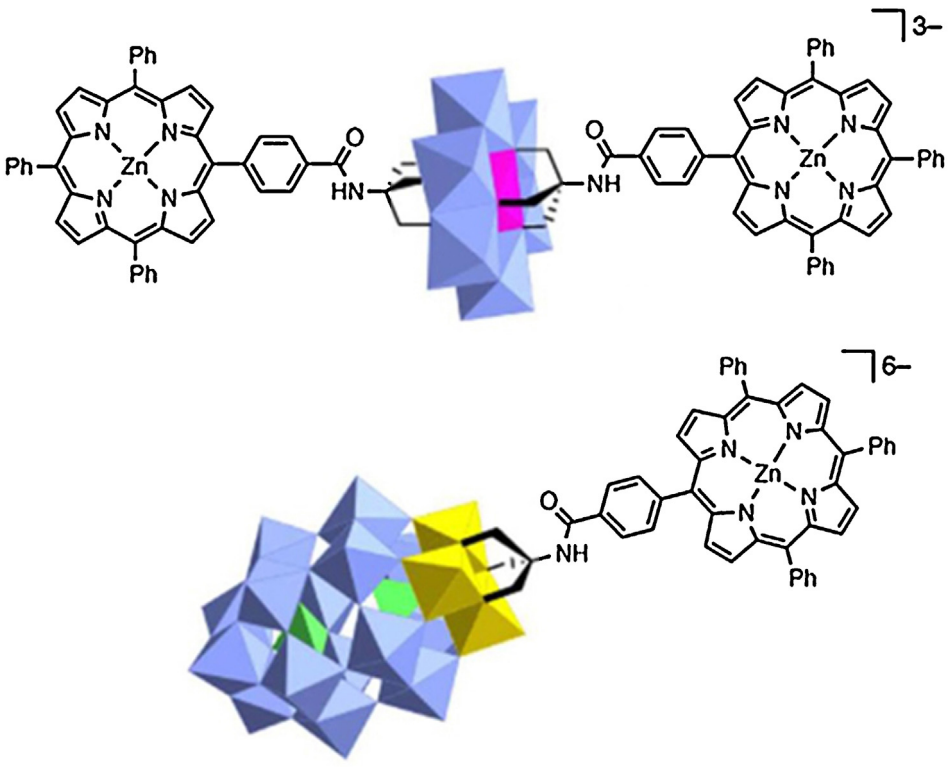

Fig. 6. Two covalently linked porphyrin-polyoxometalate hybrids: (a) an Anderson-type hexamolybdate and (b) a Dawson-type vanadotungstate [41].

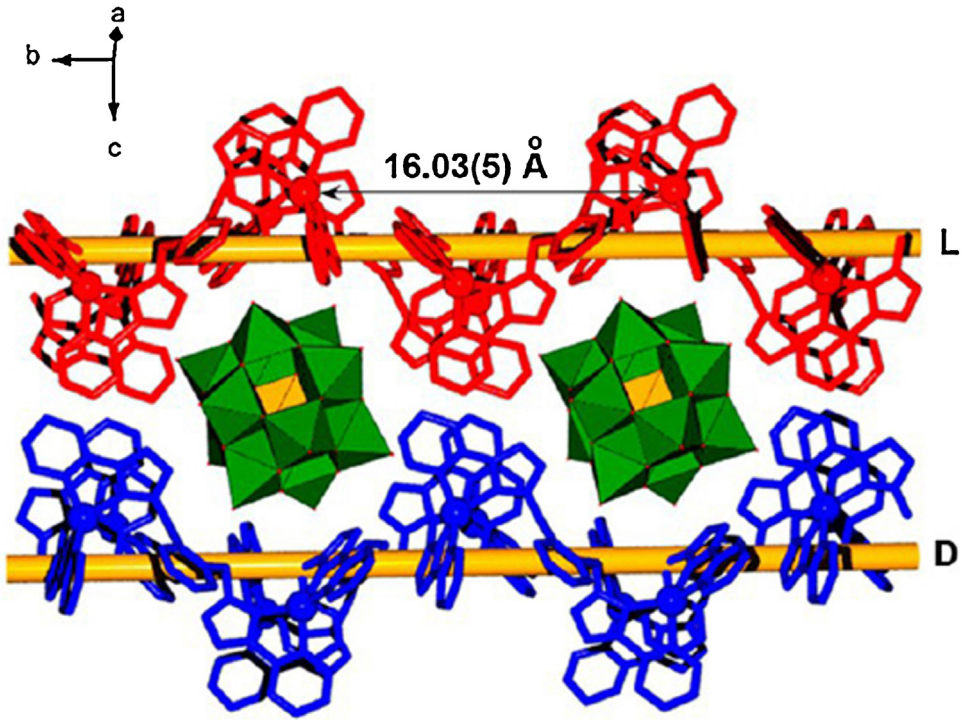

Fig. 7. Left and right helical chains arranged alternately on the *bc* plane and the central cavities occupied by the α-Keggin-type polyoxoanions [42].

comprise PCPs cations and POM anions, which play template roles in the creation of these porous structures [44]. The assembly of new Keggin POM-templated complexes has been carried out successfully in systems such as Cu/pyrazine [45], Cu/1,3,5-benzenetricarboxylate [46], Cu/tris(4-pyridyl)triazine [47], and Cu/1,1′-(1,4-butanediyl)bis-1H-benzimidazole [48]. In addition, a double-betaine-containing ligand, 1,4-bis(pyridinil-4-carboxylato)-l,4-dimethylbenzene, was used to construct a series of host lanthanide–organic frameworks that encapsulated the POM templates, with the molecular formula

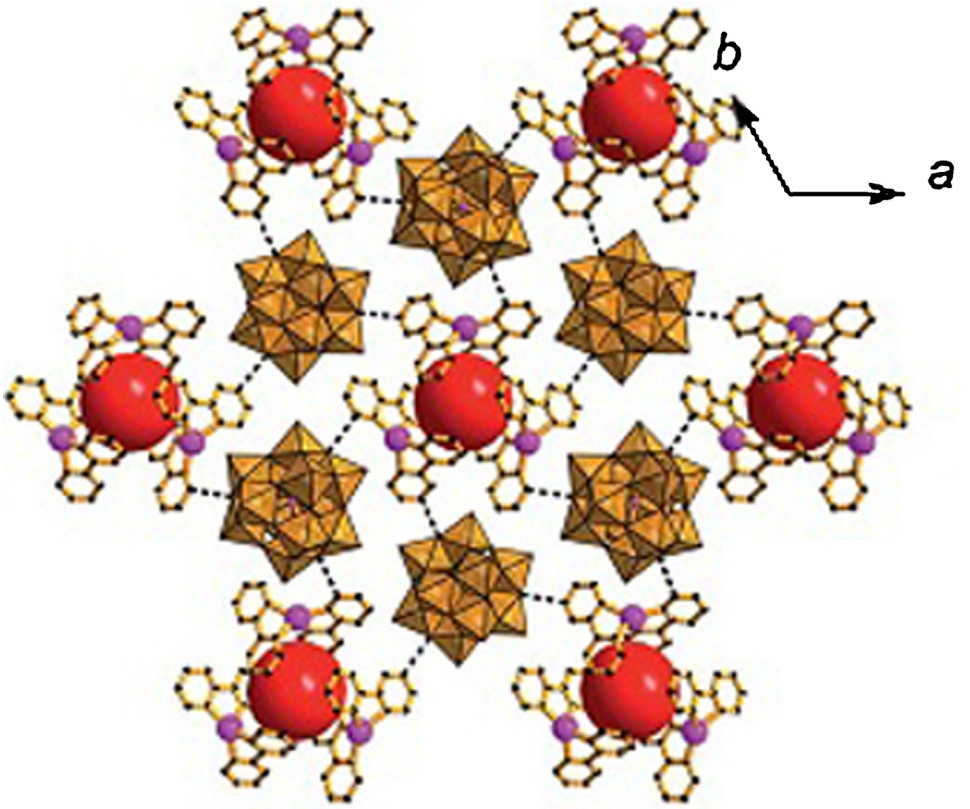

Fig. 8. The two-dimensional layer structure constructed from supramolecular cages and POMs via C—H···O hydrogen bonding interactions [43].

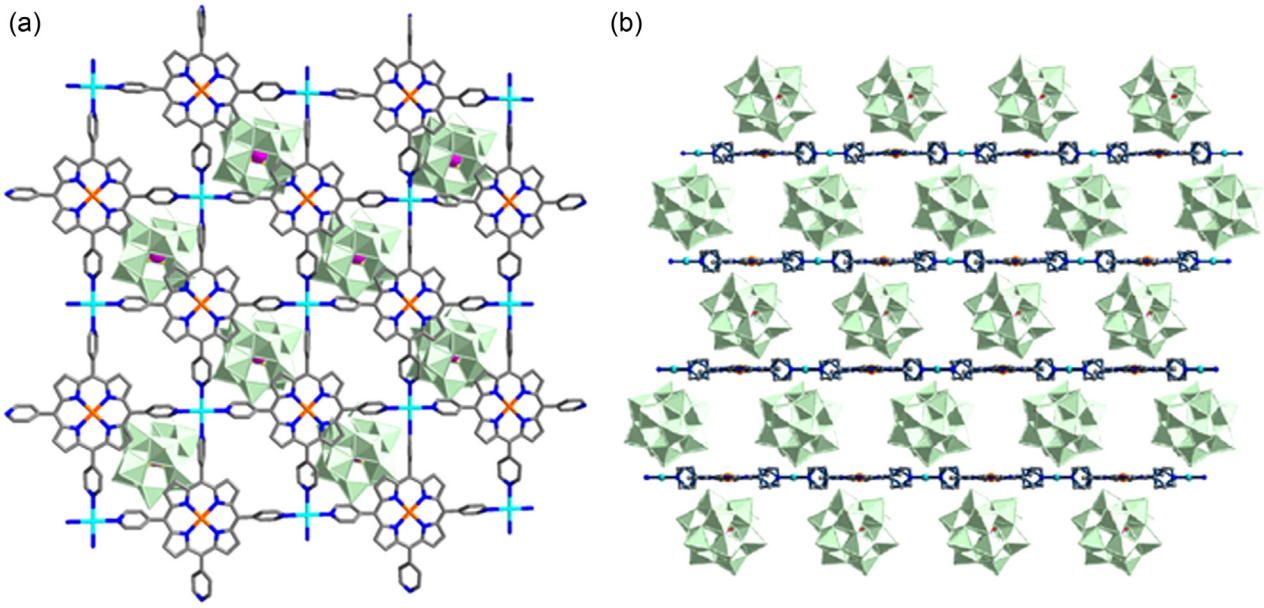

Fig. 9. Arrangement of a single layer of the lamellar framework of $[Cd(DMF)_2Mn^{3+}(DMF)_2TPyP]_n^{3n+}$ and a layer of the $[PW_{12}O_{40}]^{3-}$ polyanions, as viewed from the: (a) *c*-axis, and (b) [1 1 0] direction, where the DMF molecules and H atoms have been omitted for clarity [50].

$[Ln(L)_{1.5}(H_2O)_5][PMo_{12}O_{40}]1.5CH_3CN{\cdot}2H_2O$ (Ln = Dy, Tb and Er) [49]. These compounds are isostructural and they possess a 2D undulating cationic network $[Ln(L)_{1.5}(H_2O)_5]_n^{3n+}$ with honeycomb-like cavities. Interestingly, the 2D interval networks are also connected by hydrogen bonds to form a 3D supramolecular framework. Finally, the synthesis of porphyrin–containing POMs hybrids should be highlighted, which are generated by alternate layers of POM anions and porphyrin cationic nets [50]. Each tetrapyridylporphyrin acts as a tetradentate ligand that bridges four Cd^{2+} ions to propagate a 2D lamellar network of $[Cd(DMF)_2Mn^{III}(DMF)_2TPyP]_n^{3n+}$ parallel to the *ab* plane. The $[PW_{12}O_{40}]^{3-}$ polyanions are located between the lamellar networks (Fig. 9). The hybrid solid exhibits a remarkable capacity for scavenging dyes and for the heterogeneous selective oxidation of alkylbenzenes, with excellent product yields and 100% selectivity.

3. Coordination ability of polyoxometalates

Before starting this section, it is necessary to bear in mind that the formation of POMs involves two steps. First, the expansion of the coordination sphere of mononuclear species and second, the aggregation and condensation steps [51]. In acidic media, the protonation of $[MO_4]^{n-}$ leads to the modification of the coordination geometry of the metal, which results in the expansion of the metal coordination shell from four to six, i.e., from a tetrahedral (T_d) to an octahedral (O_h) oxygen coordination environment. This allows the protonation of the terminal oxygen atoms and facilitates condensation reactions between individual $[MO_6]$ fragments, thereby resulting in the self-assembly of larger structures in solution. Up to ten protonations and 12 water condensations are required stoichiometrically to obtain the $[XM_{12}O_{40}]^{n-}$ Keggin anion. Typically, heteropolyanions are obtained from the acidic polycondensation of $[MO_x]$ fragments around a central heteroelement, which behaves as a template. Therefore, the resulting symmetry and geometry depend strongly on the coordination geometry of the heteroanions. For example, in general POM reaction conditions, the B heteroatom tends to be trigonal, whereas Si, Ge, and P adopt a tetrahedral geometry, and transition metals such as Mo, W, Co, and Ni tend to be octahedral. The synthesis process is complicated and it depends on the ratio of M: X in solution. Recently, Bo and Poblet reported a related theoretical study that addressed POMs and the basicity of the oxo sites [52]. It is well-known that there are two main structural types of accessible oxygen atoms in POMs: bridging (M—O—M) and terminal (M=O) sites. Mapping the electrostatic potential helps to rationalize the sites that can be protonated easily, as shown in Fig. 10.

In the context of Keggin structures, molybdates are generally more basic than the homologous tungstates, i.e., by 5–10 Kcal mol^{-1} toward electrophilic ions, like protons or ammonia. In the absence of solvent effects, it has been suggested that the behaviors of molybdate and tungstate Keggin anions are quite different. The former compound has a higher tendency to be protonated in the μ_2-oxo bridging oxygen atoms, whereas the latter preferentially locate the protons in terminal oxygens. However, the inclusion of the external crystal field in the calculations may reverse the gas phase results, thereby indicating that the bridging-terminal oxygens relative basicity in POMs may be affected by their environment, which is why we observed their dynamic nature with a seemingly endless structural diversity in different systems. As mentioned earlier, POMs can act as the multidentate ligands of other transition metal ions by tuning their electronic properties

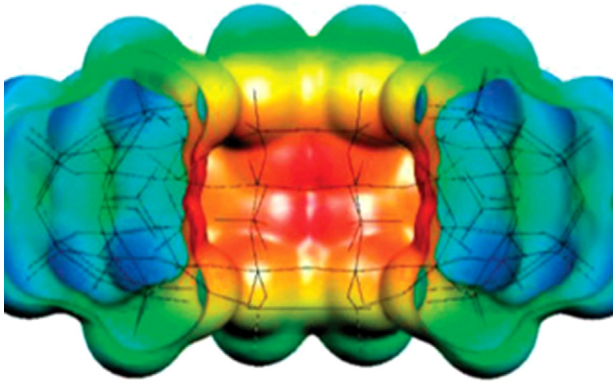

Fig. 10. Computed molecular electrostatic potentials for the internal region of the wheel-like $[P_8W_{48}O_{184}]^{40-}$. The most nucleophilic regions are indicated in red and the least in blue [52].

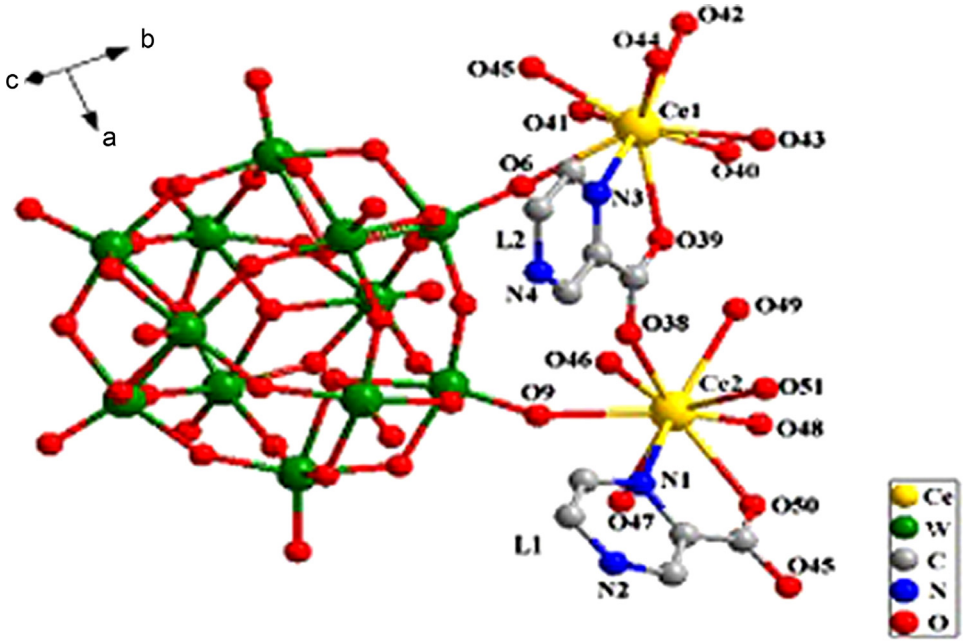

Fig. 11. Ball-and-stick representation of the asymmetric unit of the compound $(NH_4)_2[Ce_2(L)_2(H_2W_{12}O_{40})(H_2O)_7]\cdot 9H_2O$ (hydrogen atoms, ammonium ions, and crystal water molecules are omitted for clarity) [58].

and reactivity. This is attributable to the nucleophilic character of the oxygen atoms localized on the surface of the POMs, which can lead to covalent interactions with electrophilic groups. They can adopt 1–12 connecting modes via their terminal or bridging oxygen atoms, which may be symmetrical or asymmetrical, although asymmetrical surface modifications of POMs are rare and also attractive [53–57]. Compared with organic ligands, POMs have relatively weak coordination abilities. Indeed, the outer oxo groups of POMs are passivated by highly inward polarization, especially with heteropolyanions, so the coordination bonds of POMs are often weaker [44]. Thus, we can see that polyoxotungstates are less basic and more robust than POMs, because they have more ionic bonds with oxo groups. For example, in the compound $(NH_4)_2[Ce_2(L)_2(H_2W_{12}O_{40})(H_2O)_7]\cdot 9H_2O$ (L = 2-pyrazinecarboxylate), there are two crystallographically independent CE atoms, Ce1 and Ce2, which are nine-coordinated with a distorted tricapped trigonal prism coordination geometry [58]. As shown in Fig. 11, both Ce atoms are coordinated with three types of O-donor ligands, i.e., the carboxyl oxygen atoms of 2-pyrazinecarboxylate, terminal oxygen atoms of the Keggin anion, and coordination water molecules. The Ce—O distances are in the following order: Ce—O(H_2O) > Ce—O_t > Ce—O(L), therefore the electron-donating ability of the oxygen atoms in the three types of O-donor ligands is in the order: O(L) > O_t > O(H_2O). Furthermore, the Ce—O(L) bonds are more stable than the Ce—O(H_2O) and Ce—O_t bonds. A remarkable feature of this compound is that each $[H_2W_{12}O_{40}]^{6-}$ (abbreviated as W12) cluster acts as a pentadentate bridging linker, which is rare (see Section 4.1 for more examples of O-donor ligands).

An interesting compound with an N-donor ligand is $[Cu^I(bix)]_2[Cu^I(bix)](bix)[PMo_{12}O_{40}]\cdot 4H_2O$ (bix = 1,4-Bis(imidazol-1-ylmethyl)benzene), where the Keggin anion behaves as a bidentate ligand [59]. The structure is shown in Fig. 12a where it can be observed that there are two crystallographically independent Cu^+ ions (Cu1 and Cu2) and three types of bix ligands in the structural unit of this compound. The Cu1 cation is coordinated with two nitrogen atoms (Cu1–N1 = 1.873(9) Å) from two bix ligands to generate the TMC $[Cu1(bix)]_n^{n+}$, where each Cu2 cation is three-coordinated by two different nitrogen atoms (Cu2–N5 = 1.879(1) and Cu2–N4 = 1.876(1) Å) that belong to two bix ligands and one terminal oxygen atom from the $[PMo_{12}O_{40}]^{3-}$ anion (Cu2–O15 = 2.845(6) Å), which exhibits a T-shaped coordination geometry. The Cu2 ion links the bix ligands to form a one-dimensional (1D) ladder-like chain (Fig. 12b). When compared with the Cu–O15 bond length (with POM anion) with a typical Cu–O distance (ca 2.00 Å), we can confirm the weaker coordination ability of POMs.

As mentioned earlier, the coordination modes of POMs depend greatly on their environment and hybrid compounds with coordination modes of one [60,61], two [62–64], three [54–57,65,66], four [67–69], five [58], six [70–72], seven [73], eight [73–76], 10 [77–79], 11 [80], and 12 [76] are known for Keggin-type POMs. In general, odd numbers of coordination modes are less abundant, which is always expected in nature. Higher coordination modes have been achieved using Keggin-type POMs with a higher negative density charge on the cluster surface, which favors the coordination with metal cations and provides a variety of possibilities for intermolecular linkages, such as metatungstate $[H_2W_{12}O_{40}]^{6-}$ [77–79]. Indeed, the highest coordination number reported to date for W12 is 11 [80]. A W12 anion with 11 Ag^+ ions is shown in Fig. 13, which corresponds to the compound $(NH_4)_5[Ag_5(L)_2(H_2O)_8(H_2W_{12}O_{40})]\cdot H_2O$ (L = pyridine-3,5-dicarboxylate).

Keggin-type POMs with high coordination modes are usually associated with W12, but Wang et al. recently synthesized the compound $[Ag_6Cl_2(mmt)_4(H_4SiMo_{12}O_{40})(H_2O)_2]$ (mmt = 1-methyl-5-mercapto-1,2,3,4-tetrazole), which has the highest coordination number of the Keggin-type POMs produced to date [76]. Interestingly, each $[SiMo_{12}O_{40}]^{4-}$ in this compound is connected to 12 Ag^+ ions in the 3D host framework (Fig. 14).

One of the most fascinating coordination modes of the $[PMo_{12}O_{40}]^{3-}$ anion was reported by Sha et al. [81], where the crystal structure analysis showed that the compound $H[Ag_{17}(pytz)_{12}(H_2O)_6(PMo_{12}O_{40})_2]$ (pytz = 5-(2-pyridyl)tetrazolate) comprises two crystallographically independent $[PMo_{12}O_{40}]^{3-}$ anions (POM^a and POM^b). More specifically, all six terminal oxygens of the equatorial ring of POM^a and all six terminal oxygens of the two poles of POM^b participate

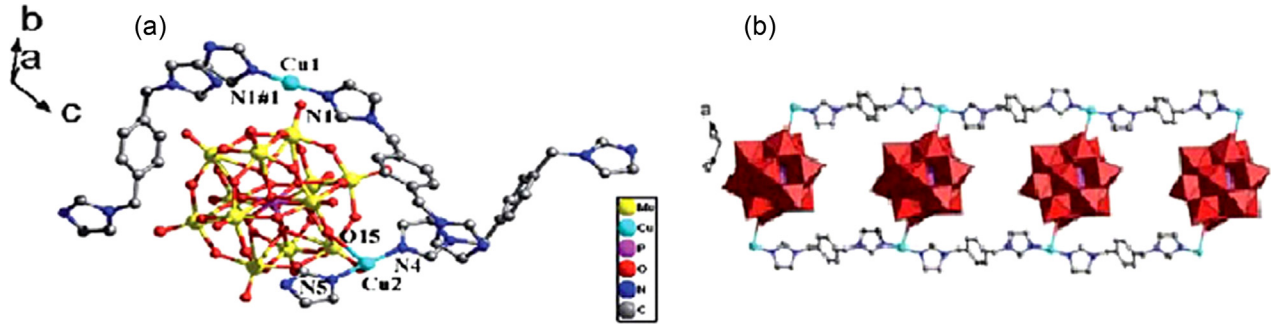

Fig. 12. (a) Ball-and-stick representation of the coordination environment of the Cu^{+} centers in the compound $[Cu^{+}(bix)]_2[Cu^{+}(bix)](bix)[PMo_{12}O_{40}]\cdot 4H_2O$. (b) Ball-and-stick and polyhedral representation of the one-dimensional chain in the structure [59].

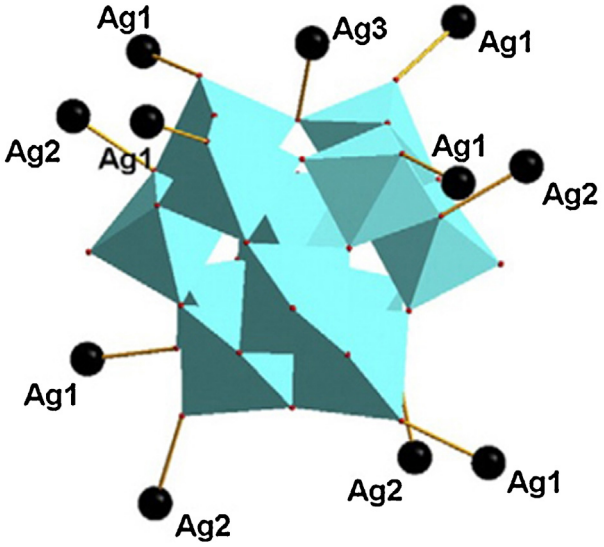

Fig. 13. View of the coordination details for W12 clusters [80].

in the coordination with Ag^{+} ions, which exhibit a complementary coordination mode with all 12 terminal oxygen atoms of the Keggin POM (Fig. 15).

Finally, as a general rule of thumb, a POM has a higher coordination mode when the positive charge of the metal complex is higher and the negative charge of the POM is higher, thus products with higher dimensionality may be achievable.

4. Ligand families

In the last decade, many efforts have been made to develop POM-based organic–inorganic hybrids to understand their capacities for constructing high-dimensional architectures. The majority of these studies have used N-donor heterocycle ligands. In this section, we consider three ligand families, i.e., pyridine dicarboxylic acids, N-oxides, and Schiff base donor ligands, which are particularly relevant to coordination chemistry. Curiously, few studies have addressed the crystal engineering of POM species and these ligands. Therefore, this particular field of research is expected to be a growth area for many investigators.

A list of compounds related to our discussion is presented in Table 1, which shows some of their structural features with respect to the behavior of the POMs. Some of these features are then discussed in more detail.

4.1. Pyridine dicarboxylic acids

A remarkable multidentate ligand family that contains two types of coordinating atoms (O and N) is formed by N-heterocyclic carboxylate ligands such as pyridine carboxylic acids, pyridine dicarboxylic acids, and pyrazine dicarboxylic acids. In recent years, these ligands have attracted much attention for the construction of POM-based hybrids because they are very useful multifunctional linkers that exhibit various coordination modes.

Table 1 suggests that lanthanides are good candidates for this type of ligand because they are prone to forming high-dimensional and unusual architectures due to their higher coordination number, more flexible coordination geometry, and stronger oxophile

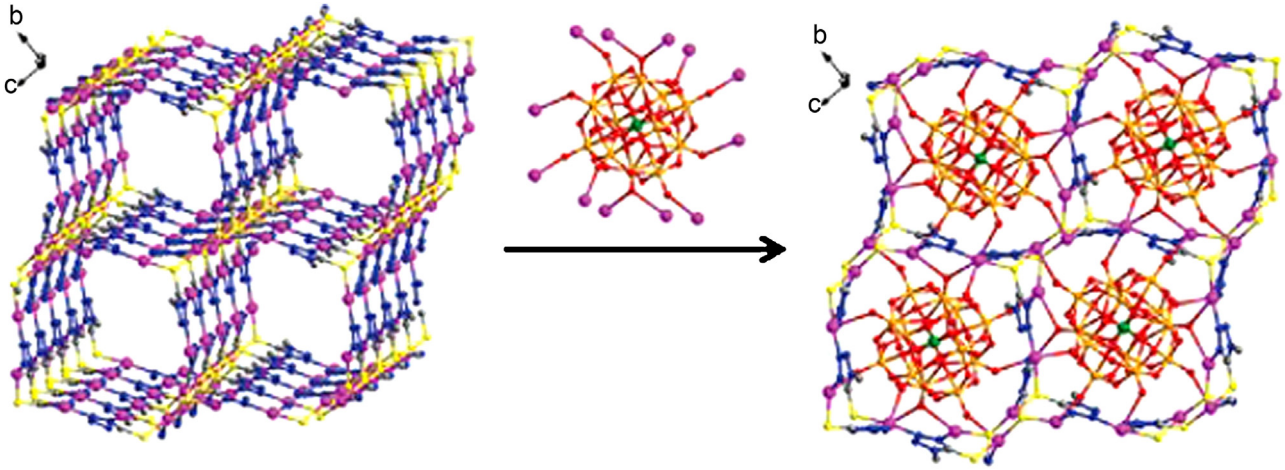

Fig. 14. Three-dimensional framework and the large dimension channels occupied by $[SiMo_{12}O_{40}]^{4-}$ polyanions [76].

Table 1
List of compounds discussed in Section 4.

Entry	Ligand[a]	POM	Metal ion	Structural features[b]	Comments	Ref.
1	4-Hydroxy-2,6-pydc	$[SiW_{12}O_{40}]^{4-}$	La, Ce, Eu	Keggin anion that acts as a tri-connected inorganic linkage by providing three terminal oxygen atoms, which belong to a single W_3O_{13} triad, for linking the trinuclear cluster $\{Na(H_2O)_3[Ln(L)(H_2O)_3]_3\}^{4+}$	First POM-based inorganic–organic assemblies using chelidamic acid as an organic ligand	[57]
2	2,6-pydc	$[SiW_{12}O_{40}]^{4-}$	Lu	Keggin anion that connects the coordination cation $\{Na(H_2O)_3[Lu(pydc)(H_2O)_3]_3\}^{4+}$ via three terminal O atoms, thereby yielding an intriguing strawberry-like structure		[56]
3	2,6-pydc	$[SiW_{12}O_{40}]^{4-}$	Ce	Keggin anion that acts as a bidentate ligand by connecting positively charged two-dimensional Ce-pdc sheets		[83]
4	2,6-pydc	$[SiW_{12}O_{40}]^{4-}$ $[SiW_{12}O_{40}]^{4-}$ $[SiMo_{12}O_{40}]^{4-}$ $[GeMo_{12}O_{40}]^{4-}$ $[SiMo_{12}O_{40}]^{4-}$ $[PMo_{12}O_{40}]^{3-}$	La, Ce, Nd Eu, Gd, Tb, Dy La, Ce, Nd Sm La	Encapsulated Keggin anion that serves as a noncoordinating guest in the tetranuclear and octanuclear cyclic units of the three-dimensional lanthanide–pdc-based host framework of $[Ln(pdc)(H_2O)_4]^+$	Compounds are isostructural Presence of one F^- anion in the starting material NaF	[83] [84] [85] [86] [86]
		$[PMo_{11}VO_{40}]^{4-}$ $[HPMo_{10}V_2O_{40}]^{4-}$	La, Ce, Pr, Nd, Sm La, Ce			[87]
5	2,6-pydc	$[PW_{12}O_{40}]^{3-}$	Ce	Keggin anion that employs two terminal oxygen atoms in the sameW3O13 group to link two Ce atoms into a three-dimensional pillar-layered structure		[88]
6	2,3-pydc	$[SiW_{12}O_{40}]^{4-}$ $[H_2W_{12}O_{40}]^{6-}$	Ag	Keggin anion that serves as a tetradentate ligand to bridge Ag atoms in two two-dimensional layers with its four terminal oxygen atoms W12 cluster that connects five Ag ions and three K ions, which act as an octadentate bridging linker ligand in $(NH_4)_4[KAg_2(Hpydc)(H_2O)_{4.5}(H_2W_{12}O_{40})]\cdot 4H_2O$		[89]
7	2,3-pzda	$[SiW_{12}O_{40}]^{4-}$	Cu	Keggin anions that are considered as templates in the $[Cu_4(pz)_6]^{4+}$ framework	In situ decarboxylation of pyrazine-2,3-dicarboxylic acid to pyrazine in the products	[90]
			Ag	Keggin anion that acts as a tetradentate ligand, which links to four $[Ag\text{-}pz]^+$ fragments		
8	2,3-pzda	$[PW_{12}O_{40}]^{3-}$	Na	Keggin anion that is covalently linked with hexanuclear $[Na_6(H_2pzdc)_6(pzdc)_2]_2^+$ macrocations, which adopt a variety of coordination modes	First two-dimensional covalent framework, with double POM anions as coordinating template	[91]
9	2,5-pydc	$[\alpha\text{-}PW_{11}O_{39}]^{7-}$	La, Ce, Pr	Unusual three-dimensional framework that comprises one $\{Ln(H_2L)_{0.5}(PW_{11}O_{39}H)\,Ln(H_2O)_4\}_2$ subunit and two similar $\{Ln(HL)(L)(H_2O)_6\}$ fragments Apart from the vacant sites of the polyoxoanions, $(\alpha\text{-}PW11O_{39})^{7-}$ is occupied by one Ln cation and the polyoxoanion coordinates with four La cations and with five Ce or Pr cations	Starting material is $K_3[\alpha\text{-}PW_{12}O_{40}]\cdot nH_2O$, but the products contain monolacunary tungstophosphate	[92]
10	2,6-pydc	$[H_2W_{12}O_{40}]^{6-}$	La, Pr, Ce, Nd	W12 cluster that acts as a tetradentate ligand, which connects four La^{3+} ions with its four terminal oxygen atoms W12 cluster as a hexadentate bridging ligand that links five La^{3+} ions	Two compounds with different structures obtained in the same solution systems	[93]
11	2,6-pydc	$[H_2W_{12}O_{40}]^{6-}$	Sm, Gd	W12 anion that connects as a tetradentate ligand to Ln_4-rings		[94]
12	3,5-pydc	$[H_2W_{12}O_{40}]^{6-}$	Tm, Yb, Lu Eu, Gd, Dy, Tb Er	W12 anion that acts as a tridentate ligand via its three terminal oxygen atoms to connect three Ln^{3+} ions	Compounds are isostructural Compounds are isostructural	[95] [96] [95]
13	3,5-pydc	$[H_2W_{12}O_{40}]^{6-}$	Ag	W12 anion connected to 11 Ag^I ions	Highest connected number for W12 reported to date See Section 3	[80]
14	2-pzc	$[H_2W_{12}O_{40}]^{6-}$	Ce, Pr, Nd, Sm	W12 anion that acts as a pentadentate bridging linker	See Section 3	[58]

Table 1 (*Continued*)

Entry	Ligand[a]	POM	Metal ion	Structural features[b]	Comments	Ref.
15	3-pyc	$[H_2W_{12}O_{40}]^{6-}$	Ag	W12 anion connected to 10 Ag centers		[78]
16	4-pyc	$[H_2W_{12}O_{40}]^{6-}$	Ce, Pr, Nd	W12 anion that coordinates with four Ln^{3+} ions as a tetradentate ligand		[97]
17	3-pyc	$[H_2W_{12}O_{40}]^{6-}$	Ag	W12 anion connected to 10 Ag fragments	The use of isomeric ligands	[79]
	4-pyc			W12 anion connected to six Ag fragments and two Na^+ ions		
18	4,4′-bpdo	$[PW_{12}O_{40}]^{3-}$	Co, Ni	Keggin anions that are considered as templates in $[M(bpdo)_3]_n$ frameworks (M = Co, Ni)	A trapped $H^+(H_2O)_{27}$ cluster in the three-dimensional MOF	[98] [99]
19	4,4′-bpdo	$[H_2W_{12}O_{40}]^{6-}$	Ce, Nd	W12 cluster connected to one $[Ce(Hdpdo)_2(H_2O)_6]^{5+}$ complex as a pendant		[61]
20	4,4′-bpdo	$[GeMo_{12}O_{40}]^{4-}$ $[GeW_{12}O_{40}]^{4-}$	Mn	Keggin anion that acts as a counterion with $[Mn(dpdo)_2(H_2O)_3]^{2+}$		[102]
21	bppdo	$[PW_{12}O_{40}]^{3-}$	Cu	Encapsulated Keggin anion as a noncoordinating guest in the $[Cu(bppdo)(Hbppdo)(CH_3CN)_3]$ ring-connected-ring chains of Cu		[103]
22	2,2′-bpdo	$[PW_{12}O_{40}]^{3-}$	Co	Encapsulated Keggin anion as a noncoordinating guest in the $[Co(2,2'\text{-bpdo})_3]$ windstick-type units of Co		[103]
23	dmbpdo	$[PMo_{12}O_{40}]^{3-}$	Dy, Tb, Er, Ho	Each isolated $[Ln(dmbpdo)_4]^{3+}$ moiety is encapsulated in a quasi-octahedral cavity constructed by eight Keggin-type polyoxoanions		[104]
24	Salen I	$[PMo_{12}O_{40}]^{3-}$ $[PW_{12}O_{40}]^{3-}$	Mn	Keggin anion bonded to one $[Mn(salen)(CH_3OH)]$ fragment via one terminal oxygen atom, which interacts with the other two $[Mn(salen)(CH_3OH)(H_2O)]^+$ fragments via electrostatic forces		[105]
25	Salen II	$[SiW_{12}O_{40}]^{4-}$	Mn	Keggin anion that acts as a counterion with $[Mn_2]^{2+}$ dimers		[106]
26	5-MeOsaltmen	$[SW_{12}O_{40}]^{2-}$	Mn	Keggin anion that acts as a counterion with $[Mn_2]^{2+}$ dimers		[106]
27	5-Brsaltmen	$[SiW_{12}O_{40}]^{4-}$	Mn	Keggin anion that connects two Mn^{III} moieties via two terminal oxygen group		[106]
28	L′[c]	$[PMo_{12}O_{40}]^{3-}$ $[PW_{12}O_{40}]^{3-}$	Ag	Keggin anion that acts as a counterion with Ag-L-chains, which exhibit three-dimensional supramolecular networks		[107]
29	bpmh	$[PW_{12}O_{40}]^{3-}$ $[PMo_{12}O_{40}]^{3-}$	Ag	Keggin anions that are considered as templates in a multinuclear Ag framework		[108]
30	bpmh	$[SiMo_{12}O_{40}]^{4-}$	Ag	Keggin anion that serves as a bidentate ligand for two $[Ag_2(bpmh)(CH_3CN)_3]^{2+}$ fragments in two opposite positions		[108]

[a] *Abbreviations*: pydc, pyridine dicarboxylic acid; pyc, pyridine carboxylic acid; pzda, pyrazine dicarboxylic acid; pzc, pyrazine carboxylic acid; bpdo, bipyridine-N,N′-dioxide; bppdo, 1,3-bis(4-pyridyl)propane-N,N′-dioxide; dmbpdo, 4,4′-dimethyl-2,2′-bipyridyl-N-N′-dioxide; salen I, N,N′-bis(salicylidene)-1,2-cyclohexanediamine; salen II, N,N′-ethylenebis-(salicylideneimine); 5-Rsaltmen, N,N′-(1,1,2,2-tetramethylethylene)bis(5-R-salicylideneimine) with R, MeO, Br; L′, 2,5-bis(3-pyridyl)-3,4-diaza-2,4-hexadiene, 1,4-bis(3-pyridyl)-2,3-diaza-1,3-butadiene, 2,5-bis(4-pyridyl)-3,4-diaza-2,4-hexadiene, and 1,4-bis-(4-pyridyl)-2,3-diaza-1,3-butadiene; bpmh, N,N′-bis-pyridin-2-ylmethylene-hydrazine.

[b] Structural features based on POM behaviors.

[c] L′ is representative of a group of Schiff base ligands.

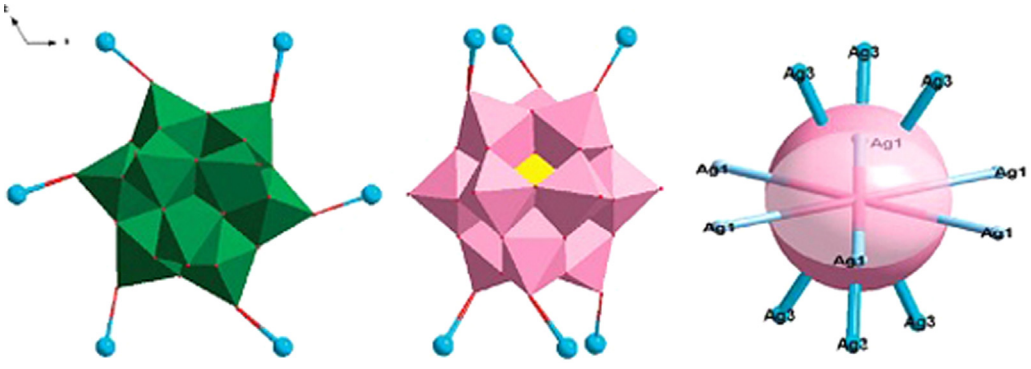

Fig. 15. The coordination modes of: (a) POM[a], (b) POM[b], and, (c) the high-point terminal oxygen coordination mode of Keggin POM [81].

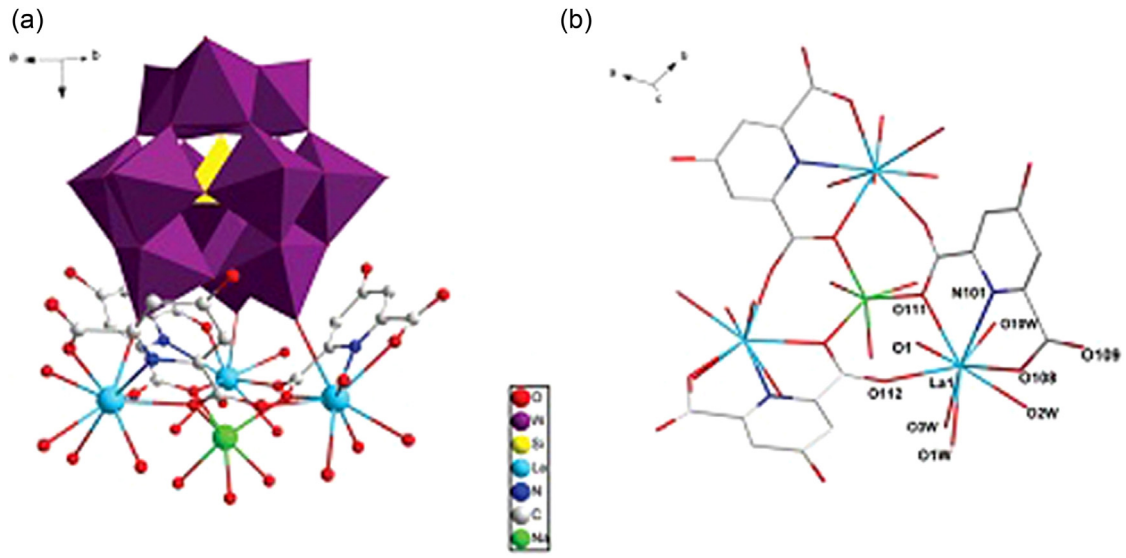

Fig. 16. (a) Ball-and-stick/polyhedral view of the molecular structure of $\{Na(H_2O)_3[La(L)(H_2O)_4]_3\}[SiW_{12}O_{40}]\cdot nH_2O$. (b) Structure of the trinuclear unit. Lattice water molecules and H atoms are omitted for clarity [57].

ability. In addition, aromatic polycarboxylic acids are particularly valuable in this context because they can act as a good bridging ligand between two lanthanide ions to enhance the weakly luminescent metal centers. In particular, when aromatic carboxylic acids are employed, they act as antenna ligands and the coordinated lanthanide ions can exhibit strong luminescence [82]. To highlight their potential, some examples from Table 1 are discussed in this section. First, our group introduced three isostructural compounds that represented the first POM-based inorganic–organic assemblies to use 4-hydroxy-pyridine-2,6-dicarboxylic acid (known as chelidamic acid) as an organic ligand. These compounds contain a polynuclear cation unit $\{Na(H_2O)[La(L)(H_2O)_4]_3\}^{4+}$ bonded to the $[SiW_{12}O_{40}]^{4-}$ polyoxoanion (Fig. 16a). Each La^{3+} ion is nine-coordinated with a monocapped square antiprism environment geometry, i.e., three carboxylate oxygen atoms from two chelidamic ligands, one nitrogen atom from the pyridine rings, one terminal oxygen atom from the Keggin, and four water molecules (Fig. 16b). Again, we can see that the average La–O_t (POM) distance is longer than the average La–O (L) distance, which indicates that the electron-donating ability of the oxygen atoms in the organic ligand is greater than the electron-donating ability of the oxygen atoms from POM molecules, while the Ln—O (L) bonds are more

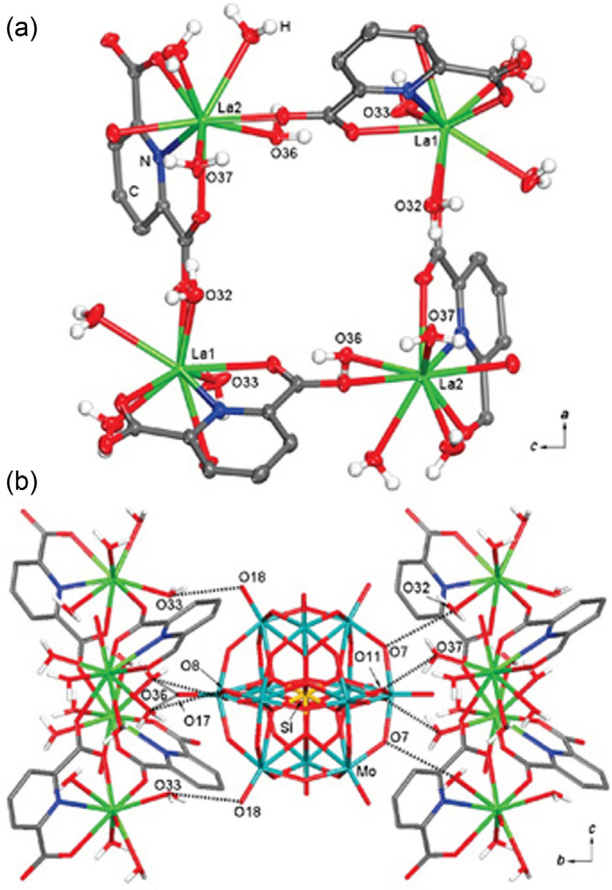

Fig. 17. (a) Structure of the tetranuclear cyclic unit in compound $\{[La(H_2O)_4(pdc)]_4\}[SiMo_{12}O_{40}]\cdot 2H_2O$. (b) View of the hydrogen bonds between two tetranuclear cyclic units $\{[La(H_2O)_4(pdc)]_4\}^{4+}$ and $[SiMo_{12}O_{40}]^{4-}$ ions [85].

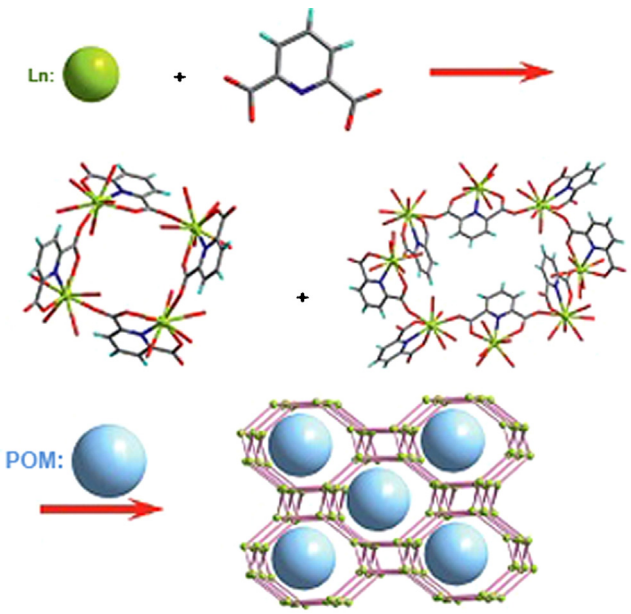

Fig. 18. Design and assembly of compounds for entry 4 [87].

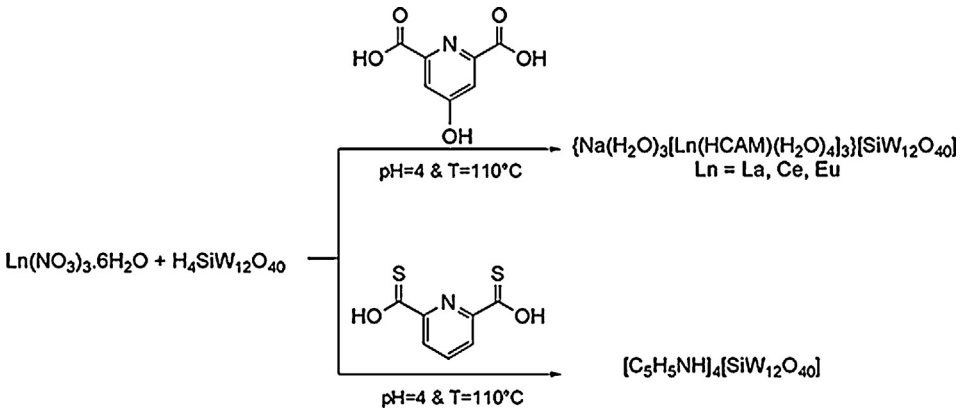

Scheme 2. Synthetic route for generating compounds derived from Keggin anions and lanthanides [57].

stable than the Ln—O_t (POM) bonds (see Section 3). In particular, each chelidamic acid ligand acts as both a chelating and bridging ligand, and it binds three cations (two equivalent La^{3+} and one Na^+) in a pentadentate fashion. The $[SiW_{12}O_{40}]^{4-}$ polyanion acts as a tri-connected inorganic linkage that provides three terminal oxygen atoms to link the trinuclear cluster in an asymmetric mode. The most noteworthy structural feature of the hybrid is that all the oxo ligands belong to a single W_3O_{13} triad, which is rare (see also entry 2).

From a synthetic viewpoint, the use of pyridine-2,6-bis(monothiocarboxylate) in the same experimental conditions leads to the formation of the pyridinium salt of 12-tungstosilicate, which is formulated as $[HC_5H_5N]_4[SiW_{12}O_{40}]\cdot H_2O$ (Scheme 2). In fact, the decomposition of the ligand occurs, which demonstrates that monothiocarboxylate ligands are less stable.

For the Ce^{3+} ion, in entries 3 and 4 with the $[SiW_{12}O_{40}]^{4-}$ anion, the compounds were isolated at different pHs of 2–3 and 4.5, respectively. An intriguing feature is that the pH value strongly affects the behavior of POMs, which changes from a bidentate ligand to a noncoordinated counteranion when the pH is increased.

However, as described in Section 2.2, MOFs are good supports for immobilizing POMs by encapsulating them in cavities because of their adjustable size and shape, high stability, and high surface area. This can be illustrated using a series of isostructural compounds constructed from 2,6-pyridine dicarboxylic (pydc), $[SiW_{12}O_{40}]^{4-}$ with Ln = Dy, La, Ce, Nd, Eu, Gd, and Tb, and $XMo_{12}O_{40}{}^{n-}$ (X = Si,Ge,P) with Ln = La, Ce, and Nd, as well as the $[PMo_{12-x}V_xO_{40}]^{(3+x)-}$ (x = 1, 2) cluster with Ln = La, Ce, Pr, Nd, and Sm (entry 4). In all of these cases, the Keggin polyanions are encapsulated as noncoordinating guests in the cyclic units of the 3D lanthanide–pydc-based host framework. Specifically, the nine-coordinated La^{3+} center coordinates with one nitrogen atom in the pydc ligand, four oxygen atoms in the carboxyl groups of three different pydc ligands, and four water molecules. In a related study [86], one of the Sm^{3+} (instead of La^{3+}) ions was eight-coordinated. As shown in Fig. 17a, four La^{3+} ions are linked by the carboxylate groups of four ligands to form a tetranuclear cyclic unit, $\{[La(H_2O)_4(pdc)]_4\}^{4+}$. Two of these tetranuclear cyclic units then chelate one $[SiMo_{12}O_{40}]^{4-}$ ion via O—H···O hydrogen bonding (Fig. 17b).

Notably, an octanuclear metallamacrocycle composed of $La_8(pydc)_8$ is present in the compound (Fig. 18). The resulting 3D lanthanide–organic cationic architecture is built up from tetranuclear cyclic units and octanuclear metallamacrocycles.

The use of the Ag ion and 2,3-pyridine dicarboxylic acid in conjunction with two types of Keggin-type POMs is a good strategy for the further development of this research (entry 6). An identical procedure was used for their preparation, except $[SiW_{12}O_{40}]^{4-}$ was replaced by $[H_2W_{12}O_{40}]^{6-}$. The latter (W12) favors higher connections with the Ag^+ ion and it acts as an octadentate ligand, in contrast to $[SiW_{12}O_{40}]^{4-}$, which serves as a tetradentate ligand in this case. Remarkably, Chen et al. selected a Keggin-type POM anion and multifunctional ligand pyrazine-2,3-dicarboxylic acid to investigate the effects of the metal ions on the structures of POM-based coordination polymers, including Cu or Ag (entry 7). This example demonstrates that the role of metal ions is crucial for the final structures based on the same procedure.

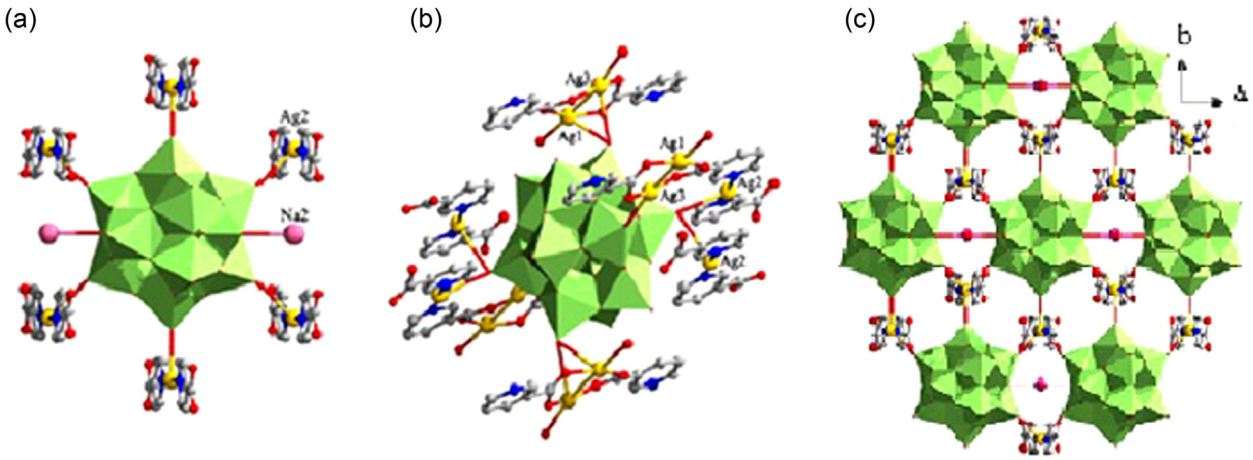

Fig. 19. Combined polyhedral/ball-and-stick representation of the connections of the W12 cluster in compound using: (a) isonicotinic acid and (b) nicotinic acid as the ligand. (c) Two-dimensional layer structure of the first structure [79].

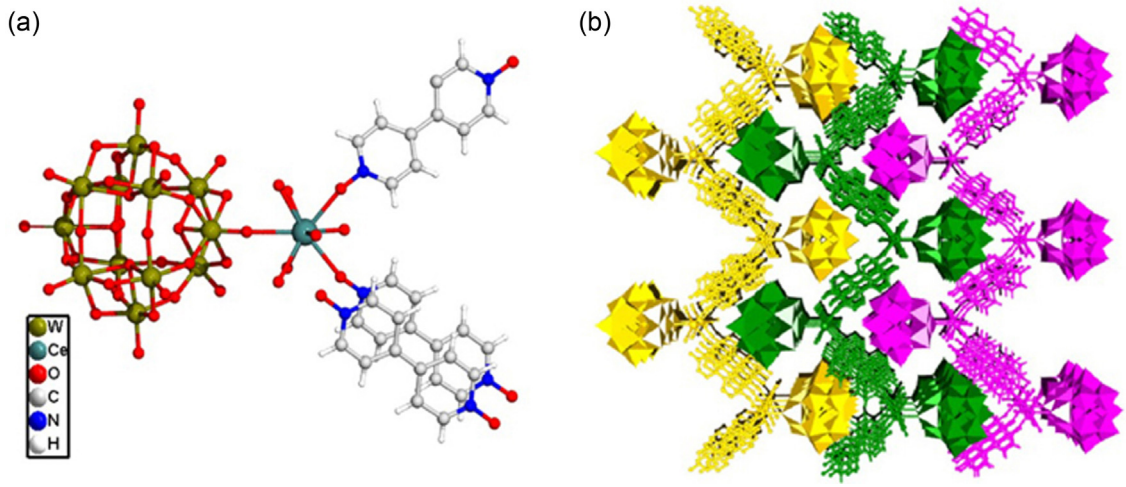

Fig. 20. (a) Fundamental unit of the compound [Hdpdo]Ln(Hdpdo)$_2$(H$_2$O)$_6$[H$_2$W$_{12}$O$_{40}$]·nH$_2$O. (b) Representation of the three-dimensional interdigitated architecture along the *a*-axis [61].

Single-crystal X-ray analysis showed that the $[SiW_{12}O_{40}]^{4-}$ moiety plays a counterion role when Cu^+ is used as the second metal ion $[Cu_4(pz)_6]^{4+}$ where it extends the 3D supramolecular structure via C—H···O hydrogen bonds and electrostatic forces, whereas its combination with the Ag^+ ion leads to the tetradentate behavior of Keggin-type POMs. Other notable features of these reactions are indicated in parentheses in Table 1. In fact, the generation of unexpected products during hydrothermal reactions is significant and pyrazine is assumed to be the in situ decarboxylation product of pyrazine-2,3-dicarboxylic acid after catalysis by a Keggin POM. In 2009, this research group also demonstrated the importance of isomeric ligands for the final structure by using different pyridine dicarboxylic acid isomers (entry 17). They demonstrated how the dimensionality increases from two to three and the connection number of the W12 cluster changes from eight to ten when the ligand is changed from pyridine-4-dicarboxylic acid (HINA) to pyridine-3-carboxylic acid (HNA) (Fig. 19a and b). In the compound $[Na_2(H_2O)_8Ag_2(HINA)_3(INA)][Na(H_2O)_2Ag_2(HINA)_4(H_2W_{12}O_{40})]\cdot 2H_2O$, each W12 cluster provides six terminal oxygen atoms from its equatorial position to covalently graft six $[Ag(HINA)_2]$ fragments and each Na atom also connects with two adjacent W12 clusters to strengthen the 2D structure (Fig. 19c).

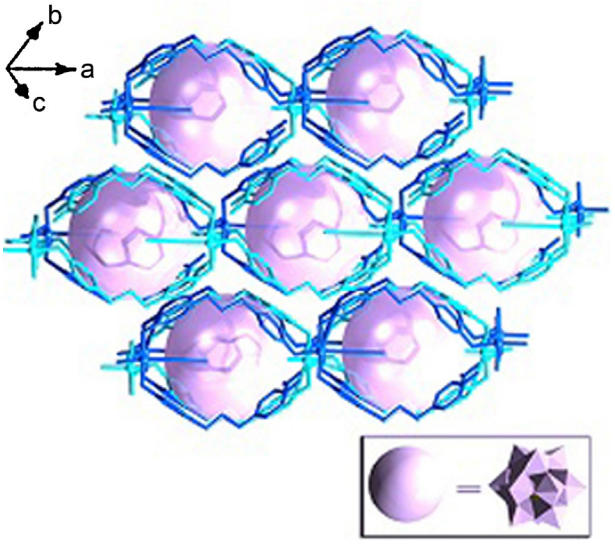

Fig. 21. Three-dimensional host–guest supramolecular network assembly of a compound derived from1,3-bis(4-pyridyl)propane-N,N′-dioxide (bppdo) [103].

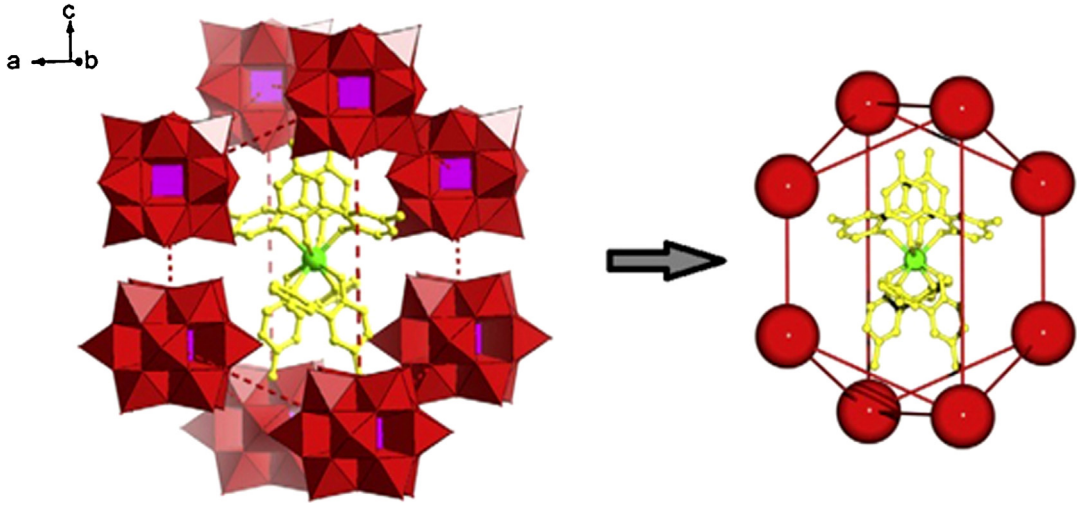

Fig. 22. Schematic view of the surroundings of an isolated $[Dy(bpyno)_4]^{3+}$ moiety constructed using eight POMs [104].

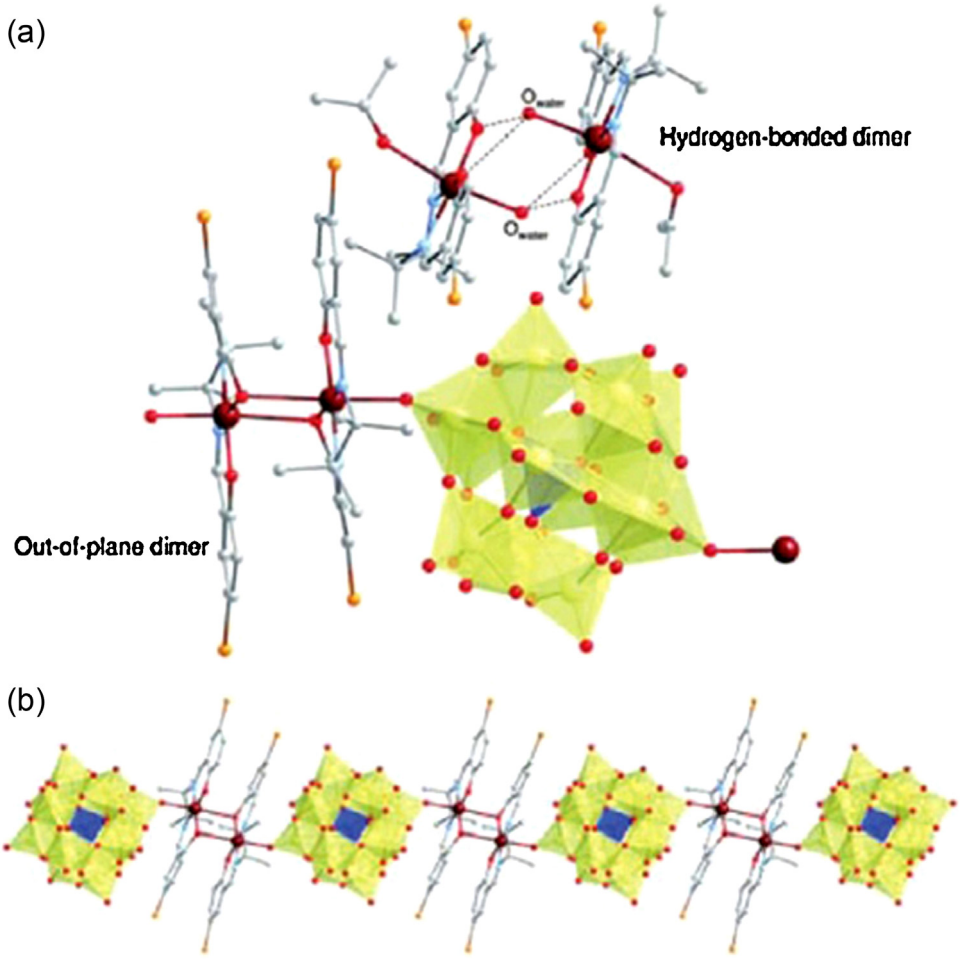

Fig. 23. (a) Structure of the formula unit and (b) the chain motif of out-of-plane dimers for $[Mn^{3+}{}_2(5\text{-Brsaltmen})_2]^{2+}$ and $[SiW_{12}O_{40}]^{4-}$ [106].

4.2. N-oxides

Ligands based on N-oxide derivatives have attracted attention in recent years because they allow the production of new architectures for POM-based hybrid inorganic–organic compounds. The most widely studied ligand is 4,4′-pipyridine-N,N′-dioxide (bpdo), which provides a long spacer that ensures high connectivity and large voids in the structure. Its use leads to the formation of robust MOFs, which can incorporate guest systems in their structure. In 2006, Duan et al. used a globular Keggin structure $[PW_{12}O_{40}]^{3-}$ anion as a template to obtain a new 3D metal–organic porous framework with the bpdo ligand. They obtained a product that acted as the host for nanometer-sized cage structures of H^+ $(H_2O)_n$ with a hydrated proton core embedded within (entry 18). X-ray analysis showed clearly that this compound, i.e., $[Co_4(bpdo)_{12}][H(H_2O)_{27}(CH_3CN)_{12}][PW_{12}O_{40}]_3$, contains cubic cavities occupied by anions and water clusters. The most fascinating feature of this compound is that a proton hydrate cluster $H^+(H_2O)_{27}$ is trapped within the 3D MOF. Later, this concept was extended to a number of Keggin-Ln-bpdo, (as well as Ni and Zn frameworks) by embedding Keggin-type polyanions within the intercrystalline voids as guests or pillars, thereby taking advantage of the good hard acid/hard base complementarity of the lanthanide cation and the N-oxide donor [99–101]. As mentioned earlier, lanthanide metals generally exhibit much higher reactivity to the oxygen atoms of POMs, which makes them favorable for producing complex and attractive structures with unique properties. One of these structures is the POM-based interdigitated architecture with lanthanide metals and bpdo ligand, which was reported recently by Ma and Pang (entry 19 in Table 1). Fig. 20a shows the fundamental unit of the two isostructural compounds, $[Hbpdo]Ln(Hbpdo)_2(H_2O)_6[H_2W_{12}O_{40}]\cdot nH_2O$ (Ln = Ce, Nd). Interestingly, the poly-pendant wave-like layers formed by discrete $\{Ln(Hdpdo)_2\ (H_2O)_6[H_2W_{12}O_{40}]\}$ fragments are stabilized by π–π interactions. Moreover, W12 clusters are ordered as pendants that are appended to wave crests via covalent bonds between the Ln cations of $Ln(Hdpdo)_2$ and the terminal oxygen atoms of W12. The adjacent layers engage in a mutual zipper-like pattern that produces a novel 3D interdigitated architecture, where the overhanging W12 clusters act as teeth (Fig. 20b).

Two POM-based coordination polymers that comprise Mn^{2+}/dpdo/$[GeM_{12}O_{40}]^{4-}$ (M = Mo, W) have also been synthesized successfully, which are basically isostructural (entry 20). In the crystal packing, Keggin anions fill the voids in the 3D network via multiform C—H···O and O—H···O hydrogen bonds. Interestingly, a pair of solvent water molecules connect two adjacent $[GeMo_{12}O_{40}]^{4-}$ anions to form a novel 1D poly-Keggin-anion chain via two types of O—H···O hydrogen bonds. Examples of N-oxides are not limited to 4,4′-bipyridine-N,N′-dioxide. Based on the aforementioned considerations, the design and synthesis of a new POM-templated host–guest hybrid (entry 21) was performed using a flexible ligand, 1,3-bis(4-pyridyl)propane-N,N′-dioxide(bppdo). The 3D host–guest supramolecular network assembly of the compound produced, $[Cu(bppdo)(Hbppdo)(CH_3CN)_3][PW_{12}O_{40}].CH_3CN\cdot 0.5H_2O$, is shown in Fig. 21. In the cationic complex fragment, each Cu^{2+}

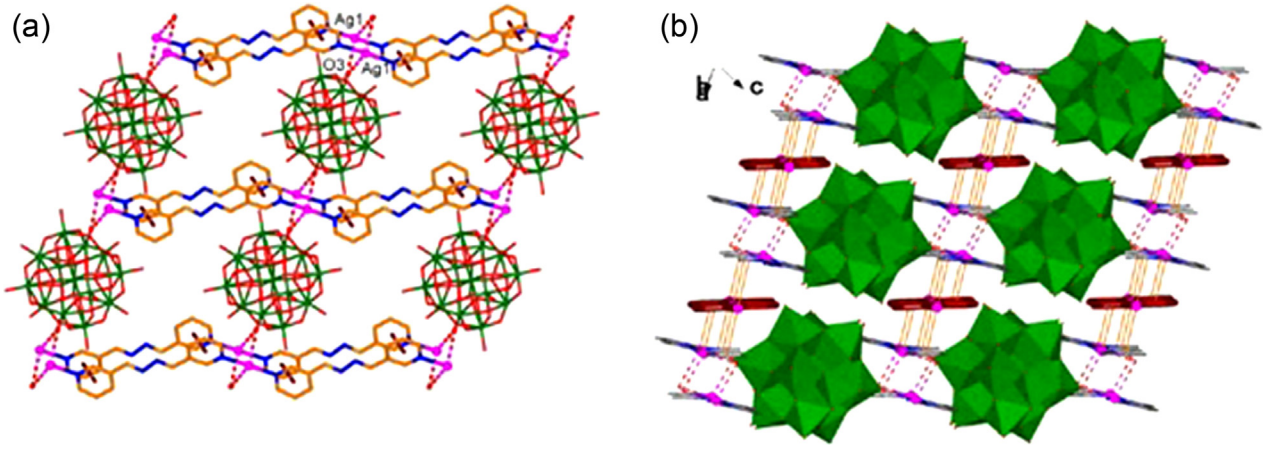

Fig. 24. (a) View of the two-dimensional structure based on Ag(1)-L-chains and $[PMo_{12}O_{40}]^{3-}$ anions, where the weak Ag···O interactions are shown by dashed lines and the π···π interactions by solid lines. (b) View of the three-dimensional supramolecular network, where the Ag···O interactions are shown by dashed lines and the Ag···π interactions by solid lines [107].

center is six-coordinated with three oxygen atoms from two different bppdo ligands and three nitrogen atoms from three different solvent acetonitrile molecules, thereby exhibiting a distorted octahedral coordination geometry. The $[PW_{12}O_{40}]^{3-}$ polyoxoanions act as guests that are encapsulated in a relatively sealed space formed by two oval rings derived from adjacent 2D supramolecular networks. In addition, the chelated ligand 2,2′-bipyridine-N,N′-dioxide(2,2′-bpdo) with the same Keggin anion produces a host-guest system that includes $[Co(2,2'\text{-bpdo})_3]$ windstick-type units (entry 22). The "guest" Keggin polyoxoanions are located in the pores and they are dispersed between two organic layers in the complex.

Furthermore, the magnetic properties of a series of isostructural compounds based on 4,4′-dimethyl-2,2′-bipyridyl-N-N′-dioxide(dmbpdo), $[Ln(dmbpdo)_4][PMo_{12}O_{40}]\cdot 2H_2O$ (Ln = Dy, Tb, Er, Ho), were probed as a new method for designing, modulating, and constructing novel single-ion magnets (entry 23). In these compounds, the mononuclear $[Ln(dmbpdo)_4]^{3+}$ units possess an approximate square antiprismatic coordination geometry and they are actually well separated by the nano-sized Keggin-type polyoxoanions, where there are no obvious intermolecular interactions between two adjacent $[Ln(dmbpdo)_4]^{3+}$ units, as shown in Fig. 22. Thus, this structural feature may allow probing of the magnetization of the cationic unit without the interference of magnetic ordering, which may facilitate exploration of the exact nature of magnetization retention by the complexes.

4.3. Schiff bases

Schiff base ligands are used widely in metal coordination chemistry, but it is surprising that little progress has been made in their use in the fabrication of POM-containing compounds. However, the limited incorporation of Schiff-base ligands in these systems has led to unprecedented and diverse topological structures. Entry 24 shows the first crystallographically characterized POM derivatives functionalized with the chiral salen–metal complex, which was reported in 2011 for a combined system of Mn^{3+}/salen/$[PM_{12}O_{40}]^{3-}$ (M = Mo, W) (salen = (−)-(R,R)-N,N′-bis(salicylidene)-1,2-cyclohexanediamine). Single-crystal X-ray diffraction analyses showed that the two compounds, formulated as $[Mn(salen)(CH_3OH)(H_2O)]_2[Mn(salen)(CH_3OH)(PM_{12}O_{40})]$, are isostructural and crystallized in the chiral space group C2. Each $[PM_{12}O_{40}]^{3-}$ anion is covalently bonded to one $[Mn(salen)(CH_3OH)]$ fragment via one terminal oxygen atom and it interacts with the other two $[Mn(salen)(CH_3OH)(H_2O)]^+$ fragments via electrostatic forces. Reactions of Mn^{3+} salen-type complexes with di ($[SW_{12}O_{40}]^{2-}$) and tetra ($[SiW_{12}O_{40}]^{4-}$) anionic Keggins were also performed by Miyasaka et al. to examine the effects of Keggin-type anions as magnetic separators in $[Mn_2]^{2+}$ dimers (entries 25–27). Interestingly, an infrequent 1D coordination polymer based on POMs emerged with a repeating unit of $[-\{Mn_2\}-POM-]_2-$ in the compound $[Mn(5\text{-Brsaltmen})(H_2O)(acetone)]_2$ $[\{Mn_2(5\text{-Brsaltmen})_2\}(SiW_{12}O_{40})]$ (5-Brsaltmen^{2-} = N,N′-(1,1,2,2-tetramethylethylene)bis(5-Br-salicylideneiminate)). According to Fig. 23, two Mn^{3+} fragments exist as monomers capped by water and acetone molecules at the axial positions, whereas the other two form an out-of-plane dimer. These dimers connect $[SiW_{12}O_{40}]^{4-}$ units via terminal oxo groups that are positioned at opposite sides of the Keggin core to form a linear 1D chain.

Moreover, the successful preparations were reported recently of a series of POM-based MOFs with silver (I)-Schiff base (L′ = derivatives of 4,4′-bipyridyl or 3,3′-bipyridyl ligands with a —CR=N—N=CR— spacer between the two pyridyl functions) coordination polymeric chains as building blocks (entry 28). The six structures constructed Exhibit 3D supramolecular networks formed by linking 1D Ag-Schiff base chains and Keggin polyoxoanion units $[PM_{12}O_{40}]^{3-}$ (M = W, Mo) via the cooperativity of multiform supramolecular interactions. The selected Ag-Schiff base system is an anion-dependent species, so the electrostatic interactions driven by the POM anions are an essential factor that affects molecular formation and crystallization. For example, a view of one of these structures, $\{[AgL]_3(PMo_{12}O_{40})\cdot(CH_3CN)_3\}_n$ [L = 1,4-bis(3-pyridyl)-2,3-diaza-1,3-butadiene], is shown in Fig. 24a. Each $[PMo_{12}O_{40}]^{3-}$ anion interconnects with four Ag(1) centers from four Ag(1)-L-chain units through two symmetrical terminal oxygen atoms μ—O where the Ag···O distances are 2.77 Å and 2.97 Å. In fact, the cooperativity of these Ag(1)—N bonds and weak Ag···O interactions helps to increase the dimensionality of the compound to form a 2D sheet. It is interesting to note that there is an obvious π–π interaction involving pyridyl rings in the adjacent Ag(1)-L-chain units. These Ag···O interactions, π–π interactions, Ag···π interactions, and hydrogen bonds link the 1D polymeric chains to form a 3D structure (Fig. 24b).

N,N′-bis-pyridin-2-ylmethylene-hydrazine (bpmh) has also been used in the synthesis of POM-based compounds with silver ions (entries 29–30). The structures of compounds that contain $[PW_{12}O_{40}]^{3-}$ and $[PMo_{12}O_{40}]^{3-}$ anions as templates comprise a 1D chain, which is constructed by the coordination of a silver center and bis-bidentate bridging ligands (Fig. 25a). By

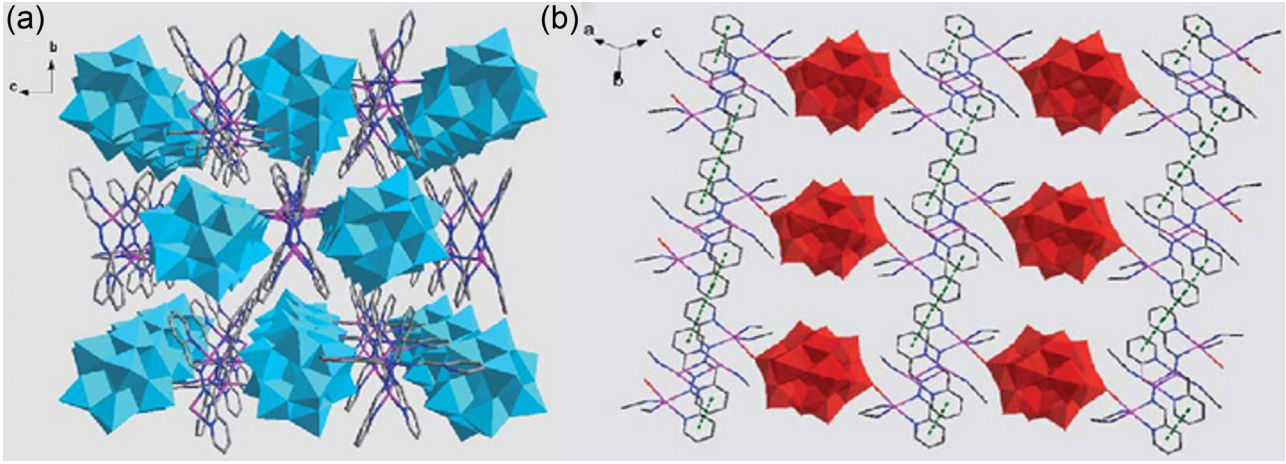

Fig. 25. (a) View of the crystal packing in $\{[Ag_3L_3](PW_{12}O_{40})(CH_3CN)(DMF)_{2.5}\}_n$. (b) View of the two-dimensional sheet in compound $[(SiMo_{12}O_{40})\{Ag_2L(CH_3CN)_3\}_2].(CH_3CN)_2$, where the π–π interactions are shown by dashed lines [108].

contrast, a compound that contains $[SiMo_{12}O_{40}]^{4-}$ exhibits a new bisupporting Keggin-POM structure, where the core supports two $[Ag_2(bpmh)(CH_3CN)_3]^{2+}$ fragments in two opposing positions (Fig. 25b).

5. Concluding remarks

In this review, we summarized recent advances in the field of POM-based inorganic–organic hybrids, where we focused on the rapid development and significant progress made in the last decade. We described the coordination ability of POMs by emphasizing their various connection modes and how they are affected by the experimental conditions. This is an interesting field of research that deserves further investigation because a diverse range of solid state architectures can be designed and synthesized by controlling the coordination ability of POMs. In the final part of this review, three different families of compounds are described, and it is expected that researchers in this field will explore the utilization of additional organic ligands to extend our knowledge of this particular area of POM chemistry.

Acknowledgments

MM and HEH would like to thank the Ferdowsi University of Mashhad for financial supporting this study (Grant no. 28395/3-2013/10/02). AF thanks the DGICYT of Spain (projects CTQ2011-27512/BQU and CONSOLIDER INGENIO 2010 CSD2010-00065, FEDER funds) and the Direcció General de Recerca i Innovació del Govern Balear (project 23/2011, FEDER funds) for financial support.

References

[1] H.N. Miras, J. Yan, D.L. Long, L. Cronin, Chem. Soc. Rev. 41 (2012) 7403.
[2] J.M. Clemente-Juan, E. Coronado, A. Gaita-Arino, Chem. Soc. Rev. 41 (2012) 7464.
[3] M. Ammam, Mater. Chem. J. A 1 (2013) 6291.
[4] D.L. Long, R. Tsunashima, L. Cronin, Angew. Chem. Int. Ed. 49 (2010) 1736.
[5] D.E. Katsoulis, Chem. Rev. 98 (1998) 359.
[6] Y.F. Song, R. Tsunashima, Chem. Soc. Rev. 41 (2012) 7384.
[7] F. Li, L. Xu, Dalton. Trans. 40 (2011) 4024.
[8] P.P. Zhang, J. Peng, H.J. Pang, J.Q. Sha, M. Zhu, D.D. Wang, M.G. Liu, CrystEngComm 13 (2011) 3832.
[9] G. Hou, L. Bi, B. Li, B. Wang, L. Wu, CrystEngComm 13 (2011) 3526.
[10] J. Niu, J. Hua, X. Ma, J. Wang, CrystEngComm 14 (2012) 4060.
[11] Y.N. Chi, F.Y. Cui, A.R. Jia, X.Y. Ma, C.W. Hu, CrystEngComm 14 (2012) 3183.
[12] A.X. Tian, J. Ying, J. Peng, J.Q. Sha, Z.M. Su, H.J. Pang, P.P. Zhang, Y. Chen, M. Zhu, Y. Shen, Cryst. Growth Des. 10 (2010) 1104.
[13] X.L. Wang, H.L. Hu, A.X. Tian, Cryst. Growth Des. 10 (2010) 4786.
[14] H. Aghabozorg, H. Eshtiagh-Hosseini, A.R. Salimi, M. Mirzaei, J. Iran. Chem. Soc. 7 (2010) 289.
[15] M. Mirzaei, H. Aghabozorg, H. Eshtiagh-Hosseini, J. Iran. Chem. Soc. 8 (2011) 580.
[16] H. Eshtiagh-Hosseini, M. Mirzaei, N. Alfi, Review on Proton Transfer Metal Complexes, LAP Lambert Academic Publishing GmbH & Co. KG, 2012.
[17] M.H. Alizadeh, H. Eshtiagh-Hosseini, M. Mirzaei, A.R. Salimi, H. Razavi, Struct. Chem. 19 (2008) 155.
[18] X.D. Yang, Y.G. Chen, M. Mirzaei, A.R. Salimi, F. Yao, Inorg. Chem. Commun. 12 (2009) 195.
[19] M. Nikpour, M. Mirzaei, Y.G. Chen, A. Aghaei-Kaju, M. Bakavoli, Inorg. Chem. Commun. 12 (2009) 879.
[20] F. Yao, Y.G. Chen, A.R. Salimi, M. Mirzaei, J. Cluster Sci. 22 (2011) 309.
[21] A. Dolbecq, E. Dumas, C.R. Mayer, P. Mialane, Chem. Rev. 110 (2010) 6009.
[22] S.X. Guo, J. Xie, R. Gilbert-Wilson, S.L. Birkett, A.M. Bond, A.G. Wedd, Dalton. Trans. 40 (2011) 356.
[23] J. Wu, G. Hu, P. Wang, F. Hao, H. Zhou, A. Zhou, Y. Tian, B. Jin, Dyes Pigments 88 (2011) 174.
[24] G. Cao, J. Xiong, Q. Xue, S. Min, H. Hu, G. Xue, Electrochim. Acta 106 (2013) 465.
[25] M.H. Alizadeh, K.T. Holman, M. Mirzaei, H. Razavi, Polyhedron 25 (2006) 1576.
[26] M.H. Alizadeh, R. Tayebee, M. Mirzaei, Cryst. Res. Technol. 43 (2008) 214.
[27] H. Eshtiagh-Hosseini, M. Mirzaei, J. Cluster Sci. 23 (2012) 345.
[28] M.H. Alizadeh, M. Mirzaei, H. Razavi, Mater. Res. Bull. 43 (2008) 546.
[29] M.H. Alizadeh, H. Eshtiagh-Hosseini, M. Mirzaei, M. Hosseini-Nejad, Polish J. Chem. 83 (2009) 1583.
[30] M. Mirzaei, H. Eshtiagh-Hosseini, M. Nikpour, A. Gholizadeh, A. Ebrahimi, Mendeleev Commun. 22 (2012) 141.
[31] M.H. Alizadeh, M. Mirzaei, A.R. Salimi, H. Razavi, Mater. Res. Bull. 44 (2009) 1515.
[32] M. Yousefi, H. Eshtiagh-Hosseini, M. Mirzaei, A.R. Salimi, M. Nikpour, Indian J. Chem. 50A (2011) 51.
[33] B. Chahkandi, M. Mirzaei, M. Chahkandi, A. Shokrollahi, F. Zarghampour, M. Shamsipour, J. Iran. Chem. Soc. 11 (2014) 187.
[34] Z. Han, T. Chai, Y. Wang, Y. Gao, C. Hu, Polyhedron 29 (2010) 196.
[35] D. Li, J. Song, P. Yin, S. Simotwo, A.J. Bassler, Y. Aung, J.E. Roberts, K.I. Hardcastle, C.L. Hill, T. Liu, J. Am. Chem. Soc. 133 (2011) 14010.
[36] M.P. Santoni, A.K. Pal, G.S. Hanan, A. Proust, B. Hasenknopf, Inorg. Chem. 50 (2011) 6737.
[37] B. Matt, C. Coudret, C. Viala, D. Jouvenot, F. Loiseau, G. Izzet, A. Proust, Inorg. Chem. 50 (2011) 7761.
[38] P. Yin, T. Li, R.S. Forgan, C. Lydon, X. Zuo, Z.N. Zheng, B. Lee, D. Long, L. Cronin, T. Liu, J. Am. Chem. Soc. 135 (2013) 13425.
[39] B. Riflade, J. Oble, L. Chenneberg, E. Derat, B. Hasenknopf, E. Lacote, S. Thorimbert, Tetrahedron 69 (2013) 5772.
[40] C.M. Drain, A. Varotto, I. Radivojevic, Chem. Rev. 109 (2009) 1630.
[41] C. Allain, D. Schaming, N. Karakostas, M. Erard, J.P. Gisselbrecht, S. Sorgues, I. Lampre, L. Ruhlmann, B. Hasenknopf, Dalton Trans. 42 (2013) 2745.
[42] X. Wang, M.M. Zhang, X.L. Hao, Y.H. Wang, Y. Wei, F.S. Liang, L.J. Xu, Y.G. Li, Cryst. Growth Des. 13 (2013) 3454.
[43] L.N. Xiao, Y. Wang, C.L. Pan, J.N. Xu, T.G. Wang, H. Ding, Z.M. Gao, D.F. Zheng, X.B. Cui, J.Q. Xu, CrystEngComm 13 (2011) 4878.
[44] R. Yu, X.F. Kuang, X.Y. Wu, C.Z. Lu, J.P. Donahue, Coord. Chem. Rev. 253 (2009) 2872.
[45] M.L. Qi, K. Yu, Z.H. Su, C.X. Wang, C.M. Wang, B.B. Zhou, C.C. Zhu, Dalton Trans. 42 (2013) 7586.
[46] F.J. Ma, S.X. Liu, G.J. Ren, D.D. Liang, S. Sha, Inorg. Chem. Commun. 22 (2012) 174.

[47] Z. Fu, Y. Zeng, X. Liu, D. Song, S. Liao, J. Dai, Chem. Commun. 48 (2012) 6154.
[48] X. Wang, J. Li, H. Lin, G. Liu, A. Tian, H. Hu, X. Liu, Z. Kang, J. Mol. Struct. 983 (2010) 99.
[49] X.L. Hao, M.F. Luo, W. Yao, Y.G. Li, Y.H. Wang, E.B. Wang, Dalton Trans. 40 (2011) 5971.
[50] C. Zou, Z. Zhang, X. Xu, Q. Gong, J. Li, C.D. Wu, J. Am. Chem. Soc. 134 (2012) 87.
[51] L. Vila-Nadal, S.G. Mitchell, A. Rodriguez-Fortea, H.N. Miras, L. Cronin, J.M. Poblet, Phys. Chem. Chem. Phys. 13 (2011) 20136.
[52] X. Lopez, J.J. Carbo, C. Bo, J.M. Poblet, Chem. Soc. Rev. 41 (2012) 7537.
[53] J.Q. Sha, J. Peng, H.S. Liu, J. Chen, A.X. Tian, P.P. Zhang, Inorg. Chem. 46 (2007) 11183.
[54] J. Sha, J. Peng, H. Liu, J. Chen, B. Dong, A. Tian, Z. Su, Eur. J. Inorg. Chem. (2007) 1268.
[55] J. Sha, J. Peng, A. Tian, H. Liu, J. Chen, P. Zhang, Z. Su, Cryst. Growth Des. 7 (2007) 2535.
[56] S. Li, D. Zhang, Y.Y. Guo, P. Ma, X. Qiu, J. Wang, J. Niu, Dalton Trans. 41 (2012) 9885.
[57] M. Mirzaei, H. Eshtiagh-Hosseini, N. Lotfian, A.R. Salimi, A. Bauza, R.V. Deun, R. Decadt, M. Barcelo-Oliver, A. Frontera, Dalton Trans. 43 (2014) 1906.
[58] H.X. Meng, Y.G. Chen, M.G. Liu, D.D. Liu, Z.C. Zhang, C.X. Zhang, S.X. Liu, Inorg. Chim. Acta 387 (2012) 8.
[59] Y. Ding, J.X. Meng, W.L. Chen, E.B. Wang, CrystEngComm 13 (2011) 2687.
[60] Y. Wang, L.N. Xiao, H. Ding, F.Q. Wu, L. Ye, T.G. Wang, S.Y. Shi, X.B. Cui, J.Q. Xu, D.F. Zheng, Inorg. Chem. Commun. 13 (2010) 1184.
[61] T. Yu, H. Ma, S. Li, H. Liu, H. Pang, Inorg. Chem. Commun. 33 (2013) 43.
[62] G. Hou, L. Bi, B. Li, L. Wu, Inorg. Chem. 49 (2010) 6474.
[63] X.Y. Wu, Q.K. Zhang, X.F. Kuang, W.B. Yang, R.M. Yu, C.Z. Lu, Dalton Trans. 41 (2012) 11783.
[64] Y. Wang, L.M. Wang, Z.F. Li, Y.Y. Hu, G.H. Li, L.N. Xiao, T.G. Wang, D.F. Zheng, X.B. Cui, J.Q. Xu, CrystEngComm 15 (2013) 285.
[65] J. Niu, J. Zhao, J. Wang, P. Ma, J. Mol. Struct. 699 (2004) 85.
[66] Y.K. Lu, X.B. Cui, Y. Chen, J.N. Xu, Q.B. Zhang, Y.B. Liu, J.Q. Xu, T.G. Wang, J. Solid State Chem. 182 (2009) 2111.
[67] X.L. Wang, J. Li, A.X. Tian, D. Zhao, G.C. Liu, H.Y. Lin, Cryst. Growth. Des. 11 (2011) 3456.
[68] X. Wang, J. Peng, M.G. Liu, D.D. Wang, C.L. Meng, Y. Li, Z.Y. Shi, CrystEngComm 14 (2012) 3220.
[69] Z.Y. Shi, Z.Y. Zhang, J. Peng, X. Yu, X. Wang, CrystEngComm 15 (2013) 7199.
[70] H.Y. Liu, H. Wu, J. Yang, Y.Y. Liu, J.F. Ma, H.Y. Bai, Cryst. Growth Des. 11 (2011) 1786.
[71] X.L. Wang, Y. Lu, H. Fu, J.X. Meng, E.B. Wang, Inorg. Chim. Acta 370 (2011) 203.
[72] J. Sha, J. Peng, Y. Zhang, H. Pang, A. Tian, P. Zhang, H. Liu, Cryst. Growth Des. 9 (2009) 1708.
[73] J.Q. Sha, J.W. Sun, C. Wang, G.M. Li, P.F. Yan, M.T. Li, M.Y. Liu, CrystEngComm 14 (2012) 5053.
[74] J.Q. Sha, J.W. Sun, C. Wang, G.M. Li, P.F. Yan, M.T. Li, Cryst. Growth Des. 12 (2012) 2242.
[75] M.G. Liu, P.P. Zhang, J. Peng, H.X. Meng, X. Wang, M. Zhu, D.D. Wang, C.L. Meng, K. Alimaje, Cryst. Growth Des. 12 (2012) 1273.
[76] X.L. Wang, Q. Gao, A.X. Tian, G.C. Liu, Cryst. Growth Des. 12 (2012) 2346.
[77] L. Lisnard, A. Dolbecq, P. Mialane, J. Marrot, F. Secheresse, Inorg. Chim. Acta 357 (2004) 845.
[78] C.J. Zhang, Y.G. Chen, H.J. Pang, D.M. Shi, M.X. Hu, J. Li, Inorg. Chem. Commun. 11 (2008) 765.
[79] C. Zhang, H. Pang, M. Hu, J. Li, Y. Chen, J. Solid State Chem. 182 (2009) 1772.
[80] Z. Zhang, Inorg. Chim. Acta 17 (2012) 38.
[81] J.Q. Sha, L.Y. Liang, J.W. Sun, A.X. Tian, P.F. Yan, G.M. Li, C. Wang, Cryst. Growth Des. 12 (2012) 894.
[82] M.L.P. Reddy, S. Sivakumar, Dalton Trans. 42 (2013) 2663.
[83] Y. Gao, Y. Xu, Z. Han, C. Li, F. Cui, Y. Chi, C. Hu, J. Solid State Chem. 183 (2010) 1000.
[84] X. Liu, Y. Jia, Y. Zhang, R. Huang, Eur. J. Inorg. Chem. (2010) 4027.
[85] C.H. Li, K.L. Huang, Y.N. Chi, X. Liu, Z.G. Han, L. Shen, C.W. Hu, Inorg. Chem. 48 (2009) 2010.
[86] X.Y. Chen, Y.P. Chen, Z.M. Xia, H.B. Hu, Y.Q. Sun, W.Y. Huang, Dalton Trans. 41 (2012) 10035.
[87] X. Lio, L. Wang, X. Yin, R. Huang, Eur. Inorg. Chem. (2013) 2181.
[88] B.F. Meng, W.S. You, X.F. Sun, F. Zhang, M.Y. Liu, Inorg. Chem. Commun. 14 (2011) 35.
[89] C.X. Zhang, Y.G. Chen, Z.C. Zhang, D.D. Liu, H.X. Meng, Solid State Sci. 14 (2012) 1289.
[90] Q. Tang, C.J. Zhang, C.H. Zhang, H.Y. Wang, Y.G. Chen, S.X. Lio, Inorg. Chem. Commun. 15 (2012) 238.
[91] H. An, T. Xu, H. Zheng, Z. Han, Inorg. Chem. Commun. 13 (2010) 302.
[92] K. Wang, D. Zhang, J. Ma, P. Ma, J. Niu, Wang, CrystEngComm 14 (2012) 3205.
[93] M.X. Hu, Y.G. Chen, C.J. Zhang, Q.J. Kong, CrystEngComm 12 (2010) 1454.
[94] X.D. Yang, C.H. Zhang, D.P. Wang, Y.G. Chen, Inorg. Chem. Commun. 13 (2010) 1350.
[95] D.D. Liu, Y.G. Chen, Inorg. Chim. Acta 401 (2013) 70.
[96] D.D. Liu, Y.G. Chen, C.J. Zhang, H.X. Meng, Z.C. Zhang, C.X. Zhang, J. Solid State Chem. 184 (2011) 1355.
[97] H. Pang, Y. Chen, F. Meng, D. Shi, Inorg. Chim. Acta 361 (2008) 2508.
[98] M. Wei, C. He, W. Hua, C. Duan, S. Li, Q. Meng, J. Am. Chem. Soc. 128 (2006) 13318.
[99] M. Wei, C. He, Q. Sun, Q. Meng, C. Duan, Inorg. Chem. 46 (2007) 5957.
[100] D. Dang, Y. Bai, C. He, J. Wang, C. Duan, J. Niu, Inorg. Chem. 49 (2010) 1280.
[101] Q. Han, L. Zhang, C. He, J. Niu, C. Duan, Inorg. Chem. 51 (2012) 5118.
[102] Y. Bai, M.M. Li, Y.J. Huang-Fu, D.B. Dang, Spectrochim. Acta A: Mol. Biomol. Spectrosc. 115 (2013) 690.
[103] X.J. Feng, W. Yao, M.F. Luo, R.Y. Ma, H.W. Xie, Y. Yu, Y.G. Li, E.B. Wang, Inorg. Chim. Acta 368 (2011) 29.
[104] W. Zhou, X. Feng, H. Ke, Y. Li, J. Tang, E. Wang, Inorg. Chim. Acta 394 (2013) 770.
[105] X. Meng, C. Qin, X.L. Wang, Z.M. Su, B. Li, Q.H. Yang, Dalton Trans. 40 (2011) 9964.
[106] Y. Sawada, W. Kosaka, Y. Hayashi, H. Miyasaka, Inorg. Chem. 51 (2012) 4824.
[107] D. Dang, Y. Zheng, Y. Bai, X. Guo, P. Ma, J. Niu, Cryst. Growth Des. 12 (2012) 3856.
[108] Y. Bai, G.Q. Zhang, D.B. Dang, P.T. Ma, H. Gao, J.Y. Niu, CrystEngComm 13 (2011) 4181.